Manuscript Details

Manuscript number	ALGAL_2017_966
Title	Transcriptome analysis reveals the genetic foundation for the dynamics of starch and lipid production in Neochloris oleoabundans
Article type	Full Length Article

Abstract

The oleaginous microalga Neochloris oleoabundans accumulates both starch and lipids to high levels under stress conditions such as nitrogen starvation (N-). To steer biosynthesis towards starch or lipids only, it is important to understand the regulatory mechanisms involved. Here physiological and transcriptional changes under nitrogen starvation were analysed in controlled flat-panel photobioreactors at both short and long time-scales. Starch accumulation was transient and occurred rapidly within 24 hrs upon starvation, while lipid accumulation was gradual and reached a maximum after 4 days. The major fraction of accumulated lipids was composed of de novo synthesized neutral lipids - triacylglycerides (TAG) - and was characterized by a decreased composition of the polyunsaturated fatty acids (PUFAs) C18:3 and C16:3 and an increased composition of the mono-unsaturated (MUFAs) and saturated (SFAs) fatty acids C18:1/C16:1 and C18:0/C16:0, respectively. RNA-sequencing revealed that starch biosynthesis and degradation genes show different expression dynamics from lipid biosynthesis ones. An immediate rapid increase in starch synthetic transcripts was followed by an increase in starch degrading transcripts and a decrease in the starch synthetic ones. In contrast, increased gene expression for fatty acid and TAG synthesis was initiated later and occurred more gradually. Expression of several fatty acid desaturase (FAD) genes was decreased upon starvation, which corresponds to the observed changes to higher levels of MUFAs and SFAs. Moreover, several homologs of transcription regulators that were implicated in controlling starch and lipid metabolism in other microalgae showed differential gene expression and might be key regulators of starch and lipid metabolism in N. oleoabundans as well. Our data provide insights into the genetic foundation of starch and lipid metabolism in N. oleoabundans under nitrogen starvation and should facilitate metabolic engineering towards tailored strains with desired storage compound composition.

Keywords	microalgae; nitrogen starvation; starch; lipids; carbon-partitioning; transcriptome
Taxonomy	Starch, Lipids, Algal Physiology, Metabolism, Algal Culture, Transcriptomics
Manuscript category	Algal Biotechnology
Corresponding Author	Mark Sturme
Corresponding Author's Institution	Wageningen Universiteit
Order of Authors	Mark Sturme, Yanhai Gong, Josué Heinrich, Anne Klok, Gerrit Eggink, Dongmei Wang, Jian Xu, Rene Wijffels
Suggested reviewers	Matthew Posewitz, Olaf Kruse, Alison Smith, Philip Pienkos

Submission Files Included in this PDF

File Name [File Type]

Cover Letter_Sturme-Gong_et-al-2017.pdf [Cover Letter]

Highlights_Sturme-Gong_et-al-2017.docx [Highlights]

Sturme_Gong_et-al_2017.docx [Manuscript File]

Acknowledgements_Sturme_Gong_et-al_2017.docx [Supporting File]

Supplementary Figure A1 - Quantum Yield.docx [Supporting File]

Supplementary Figure A2 - Sample correlation matrix.docx [Supporting File]

Supplementary Figure A3 - starch TAG content.docx [Supporting File]

Supplementary Figure A4 - GOBubble GOSlimPlant plots.docx [Supporting File]

Submission Files Not Included in this PDF

File Name [File Type]

Supplementary Figure A5 - KEGG pathway ko00020.gif [Supporting File]

Supplementary Figure A5 - KEGG pathway ko00195.gif [Supporting File]

Supplementary Figure A5 - KEGG pathway ko00500.gif [Supporting File]

Supplementary Figure A5 - KEGG pathway ko00561.gif [Supporting File]

Supplementary Figure A5 - KEGG pathway ko00564.gif [Supporting File]

Supplementary Figure A5 - KEGG pathway ko00710.gif [Supporting File]

Supplementary Figure A5 - KEGG pathway ko04141.gif [Supporting File]

Supplementary Figure A5 - KEGG pathway ko04145.gif [Supporting File]

Supplementary Table 2 - GO-terms enrichment.xlsx [Supporting File]

Supplementary Table 3 - GO-terms depletion.xlsx [Supporting File]

Supplementary Table 4 - KEGG pathways from GAGE gene set enrichment.xlsx [Supporting File]

Supplementary Table 1 - Differential Expression overview.xlsx [Supporting File]

To view all the submission files, including those not included in the PDF, click on the manuscript title on your EVISE Homepage, then click 'Download zip file'.

Research Data Related to this Submission

Data set   https://www.ncbi.nlm.nih.gov/geo/query/acc.cgi?acc=GSE104807

Time series data

RNA-seq data of individual samples from time series of Neochloris oleoabundans under nitrogen starvation.

Data set   https://www.ncbi.nlm.nih.gov/nuccore?term=GFXW00000000.1

Reference transcriptome

Reference transcriptome built by RNA-seq of RNA extracted from combined samples (both nitrogen-replete and nitrogen-depleted) from time series of Neochloris oleoabundans.

WAGENINGEN
UNIVERSITY & RESEARCH

P.O. Box 16 | 6700AA Wageningen | The Netherlands

Algal Research,

DATE
December 12, 2017

POSTAL ADDRESS
P.O. Box 16
6700AA Wageningen
The Netherlands

VISITORS' ADDRESS
Wageningen Campus
Building 107
Droevendaalsesteeg 1
6708PB Wageningen Campus

INTERNET
www.wur.nl/bpe
www.wur.nl/university

CoC NUMBER
09215846

HANDLED BY
Dr. M.H.J. Sturme

TELEPHONE
+31 317482954

EMAIL
mark.sturme@gmail.com

Dear editor of Algal Research, Dear Prof. Olivares,

Please find enclosed our manuscript entitled "**Transcriptome analysis reveals the genetic foundation for the dynamics of starch and lipid production in *Neochloris oleoabundans***" by Sturme *et al*. This is an original research article that we would like to submit to **Algal Research**. The submitted manuscript version is approved by all authors, and the authors declare no conflict of interests. Furthermore, we confirm that this manuscript was not submitted for publication elsewhere.

Neochloris oleoabundans can accumulate both starch and lipids to high levels under stress, and understanding the genetic mechanisms that govern the accumulation of storage compounds are important to steer biosynthesis to starch or lipids only. The manuscript by Sturme *et al*. highlights the analysis of the dynamics of starch and lipid accumulation and the corresponding transcriptional changes during nitrogen starvation in the microalgae *N. oleoabundans*.

Our data show that starch and lipid accumulation upon nitrogen starvation follow different dynamics: starch accumulates rapid and transiently, while lipids accumulate gradually. Accumulated lipids were mainly composed of *de novo* synthesized triacylglycerides (TAG) and characterized by a decreased composition of polyunsaturated fatty acids (PUFAs) and an increased composition of mono-unsaturated (MUFAs) and saturated (SFAs) fatty acids. Transcriptome analysis revealed different expression dynamics for starch biosynthesis and degradation genes from those of lipid biosynthesis. Starch synthetic transcripts showed an immediate rapid increase, followed by an increase in starch degrading transcripts and a decrease in starch synthetic ones. In contrast, gene expression for fatty acid and TAG synthesis increased later in starvation and occurred more gradually. Expression of fatty acid desaturase genes decreased upon starvation, corroborating the observed changes to higher MUFAs and SFAs levels. Moreover, several homologs of transcription regulators implicated in controlling starch and lipid metabolism in other microalgae showed differential gene expression and might play this role in *N. oleoabundans* as well.

This manuscript provides new insights into the genetic basis of starch and lipid metabolism in this industrially important microalga, which should facilitate metabolic engineering towards strains with desired storage compound composition. We therefore consider it to be of interest to be submitted for publication in Algal Research and are looking forward to your reply.

With kind regards,

Dr. Mark H.J. Sturme

100years
1918 — 2018

Highlights

- Starch accumulates transiently in nitrogen-starved *Neochloris oleoabundans*

- Lipids accumulate gradually in nitrogen-starved *Neochloris oleoabundans*

- Accumulated lipids are mostly composed of *de novo* synthesized triacylglycerides

- Triacylglycerides show increased mono-unsaturated and saturated fatty acid content

- Transcriptome reveals genetic mechanisms of storage compound accumulation dynamics

Transcriptome analysis reveals the genetic foundation for the dynamics of starch and lipid production in *Neochloris oleoabundans*

Mark H.J. Sturme [1, #, *], Yanhai Gong [2, #], Josué Miguel Heinrich [1], Anne J. Klok [1], Gerrit Eggink [1], Dongmei Wang [2], Jian Xu [2], Rene H. Wijffels [1,3]

[1] Department of Bioprocess Engineering/AlgaePARC, Wageningen University, The Netherlands;

[2] Single-Cell Center, CAS Key Laboratory of Biofuels and Shandong Key Laboratory of Energy Genetics, Qingdao Institute of BioEnergy and Bioprocess Technology, Chinese Academy of Sciences, Qingdao, Shandong 266101, China;

[3] Faculty of Biosciences and Aquaculture, Nord University, N-8049 Bodø, Norway

[#] Equal contribution

[*] Corresponding author: mark.sturme@gmail.com

Abstract

The oleaginous microalga *Neochloris oleoabundans* accumulates both starch and lipids to high levels under stress conditions such as nitrogen starvation (N-). To steer biosynthesis towards starch or lipids only, it is important to understand the regulatory mechanisms involved. Here physiological and transcriptional changes under nitrogen starvation were analysed in controlled flat-panel photobioreactors at both short and long time-scales. Starch accumulation was transient and occurred rapidly within 24 hrs upon starvation, while lipid accumulation was gradual and reached a maximum after 4 days. The major fraction of accumulated lipids was composed of *de novo* synthesized neutral lipids - triacylglycerides (TAG) - and was characterized by a decreased composition of the polyunsaturated fatty acids (PUFAs) C18:3 and C16:3 and an increased composition of the mono-unsaturated (MUFAs) and saturated (SFAs) fatty acids C18:1/C16:1 and C18:0/C16:0, respectively. RNA-sequencing revealed that starch biosynthesis and degradation genes show different expression dynamics from lipid biosynthesis ones. An immediate rapid increase in starch synthetic transcripts was followed by an increase in starch degrading transcripts and a decrease in the starch synthetic ones. In contrast, increased gene expression for fatty acid and TAG synthesis was initiated later and occurred more gradually. Expression of several fatty acid desaturase (FAD) genes was decreased upon starvation, which corresponds to the observed changes to higher levels of MUFAs and SFAs. Moreover, several homologs of transcription regulators that were implicated in controlling starch and lipid metabolism in other microalgae showed differential gene expression and might be key regulators of starch and lipid metabolism in *N. oleoabundans* as well. Our data provide insights into the genetic foundation of starch and lipid metabolism in *N. oleoabundans* under nitrogen starvation and should facilitate metabolic engineering towards tailored strains with desired storage compound composition.

1. Introduction

With a growing world population and declining natural oil and gas reserves, the global demand for sustainable and renewable resources becomes ever more relevant. In this respect, microalgae are a promising source for sustainable production of food additives, chemical building blocks and cosmetic ingredients. Microalgae can accumulate high levels of storage compounds such as carbohydrates, lipids and pigments under stress conditions and can serve as a renewable source of proteins. They can be cultivated on marginal lands and in (semi-)arid regions and many do not require freshwater for their growth. Thereby they do not compete with agricultural crop production or affect drinking water supply. Moreover, they are a particularly good substitute for vegetable oils since the negative environmental impact of e.g. palm, the main oil source currently used in food applications, can potentially be mitigated [1–3]. Nevertheless, the market for most microalgae-derived products currently is not economically competitive with those derived from existing plant-based and petrochemical resources. To overcome this gap, microalgal strain development in combination with improved biorefineries is required [4,5]. Many studies for microalgal strain development have focused on metabolic engineering by the introduction or mutagenesis of single target genes involved in lipid, starch or pigment biosynthesis [6,7] and less on engineering of multiple genes or complete pathways [8]. The selected gene targets for metabolic engineering have been identified by transcriptomics or were based on detailed biochemical and genetic information from other microalgal or plant models. Most of these studies focused on microalgae that accumulate only lipids or starch under stress conditions such as nitrogen or phosphorus starvation, while only a few have focused on transcriptomics and metabolic engineering of so-called "hybrid" producers: oleaginous microalgae that are capable of simultaneous accumulation of starch and neutral lipids such as triacylglycerides (TAG). The oleaginous microalgae *Neochloris oleoabundans* and *Acutodesmus obliquus* and several *Chlorella* species are known hybrid producers of industrial

3

relevance that accumulate high levels of both starch and lipids under nitrogen starvation [9–11]. For industrial applications, it would be preferred that in such hybrid producers carbon-partitioning could be altered to produce mainly TAG or starch and to genetically control the switch between starch and lipid metabolism. The genetic foundation for this dual accumulation strategy however is unknown in most of these microalgae, due to a lack of well-annotated genome sequences and a limited number of transcriptome studies. It is also plausible that the regulatory mechanisms for storage compound accumulation in hybrid producers are more complex than in microalgae mainly accumulating a single storage compound. *N. oleoabundans* is a hybrid producer with several properties that make it a very suitable candidate for industrial production. It can accumulate up to 56% of its cell dry weight as lipids under nitrogen starvation, mainly in the form of TAG, and while isolated as a freshwater strain it can also grow and accumulate storage compounds under saline conditions and high pH as well [12–15]. Furthermore, continuous TAG production in continuously growing cells has been reported [16]. However, the genomic foundation for these favourable industrial traits of *N. oleoabundans* currently is not yet established. The few studies that addressed the transcriptional changes upon nitrogen starvation in this species, have analysed either a single timepoint at an early-stage (<24 hrs) [15] or a late-stage (11 days) during batch N-starvation [17] or investigated transcriptomes during nitrogen limitation under turbidostat cultivation [18]. For a full understanding of the cellular and transcriptional changes upon N-starvation it is necessary to track the temporal dynamics of metabolite concentrations, physiological parameters and transcript abundances over both a short and long timespan, to identify key regulatory genes controlling metabolic switch-points. Some recent studies in e.g. *Chlamydomonas rheinhardtii*, *Chlorella* spp., *Nannochloropsis* spp. and *Monoraphidium neglectum* have performed this correlation analysis of storage compound accumulation and transcriptome patterns, which indicated possible transcription factors and metabolic nodes that are involved in or even control the "switch"

4

between starch and lipid metabolism [20–25]. In addition, integration of transcriptomics with genome-scale metabolic models could aid in pinpointing the critical metabolic nodes that should be targeted in metabolic engineering.

In this study, we therefore set out to perform an in-depth analysis of the temporal dynamics of storage compound accumulation and transcriptome changes during nitrogen starvation in *N. oleoabundans*, with the aim to identify the metabolic genes and transcriptional factors that are involved in the switch between starch and lipid metabolism in this microalga. Our results revealed the differences in temporal dynamics of gene expression for the starch and lipid pathways upon nitrogen starvation, and identified transcriptional regulators that might be involved. These insights are valuable for rational metabolic engineering in this important industrial microalga.

2. Materials & Methods

2.1 Culture conditions and nitrogen starvation experiment

Neochloris oleoabundans UTEX 1185 (culture collection of Algae, University of Texas, Austin) was grown in Bold's Basal Medium (BBM) at pH 7.5 and 25ºC, with 25.2 mM KNO_3 (N-replete conditions) or without nitrate (N-starvation). Experiments were performed in 1.7L flat panel air-lift photobioreactors (Labfors 5 Lux, Infors HT, Switzerland) at pH 7.5 and 25ºC, and sparged with 2% CO_2 at an air flow of 1.2 L min^{-1} and photon flux density (PFD) of 800 µmol s^{-1} m^{-2} at a 12:12 day:night cycle. A nitrogen-replete batch pre-culture of *N. oleoabundans* (250 mL) was used to inoculate the photobioreactors, and microalgae were further batch cultivated until a biomass concentration of 2 g cell dry weight (CDW)/L was reached. Subsequently, fed-batch nitrogen-replete cultivation (N+) was continued for several days until a stable biomass concentration was maintained. For the nitrogen starvation experiment biomass from the nitrogen-replete fed-batch culture was collected, spun down, rinsed and resuspended

5

in nitrogen-free BBM medium. The reactors were rinsed with distilled water, filled with nitrogen-free BBM medium and inoculated with the same volume of the collected microalgae. During the nitrogen-depleted phase (N-), the reactors were run in fed-batch mode. Medium was fed at 800 mL/d to compensate for the volume-loss due to sampling. Samples for analysis of biomass and cell parameters from the nitrogen-replete fed-batch phase (N+) were collected at four timepoints in the light-phase preceding nitrogen starvation (-25, -23, -19 and -15 hrs; Fig. 1). Samples for biomass, cell parameter and molecular analysis from the onset of nitrogen starvation (N-) were collected at time-points at the start, middle and end of each light-phase and at the end of each dark-phase over a 4-day period (0, 2, 6, 10, 23, 29, 33, 46, 53, 71, 77 and 99 hrs; Fig. 1). Samples were centrifuged, and cell pellets snap frozen in liquid nitrogen and stored at -80ºC. The experiments were performed as three biological replicates.

2.2 Biomass analysis

2.2.1 Cell dry weight, cell count and cell parameters

Cell dry weight (CDW) concentrations were determined as described by Kliphuis et al. [26], by filtering culture broth (around 10 mg of biomass) through pre-dried (100°C overnight) and pre-weight Whatman glass fibre filter paper (GF/F; Whatman International Ltd, Maidstone, UK). The filter was washed with filtered demineralized water and subsequently dried overnight at 100°C before weighing. Cell numbers were determined using a Multisizer™ 3 Coulter Counter® (Beckman Coulter). Quantum yield (QY) was determined using an Aquapen-C (Photon Systems Instruments, Czech Republic) and pigment content measured by spectrophotometric absorbance at 480, 680, and 750 nm.

2.2.2 Total fatty acids

Extraction and quantification of total fatty acids (TFA) were adapted from Breuer et al. [27]. Around 20 mg of pellet was transferred to bead beating tubes (Lysing Matrix E; MP

6

Biomedicals, Santa Ana, CA, USA) and lyophilized overnight. Freeze-dried cells were disrupted by a bead beating step in a Precellys® 24 bead beater (Bertin Technologies) for 2x (3x60sec with 120sec pause in between at 2500rpm), followed by 1x (2x60sec with 120 seconds pause in between at 2500 rpm) in the presence of a chloroform:methanol mixture (1:1.25) to extract the lipids from the biomass. The internal standards C15:0 (tripentadecanoin - T4257; Sigma-Aldrich, St Louis, MO, USA) and C19:0 (trinonadecanoin - T4632; Sigma-Aldrich, St Louis, MO, USA) were added to the extraction mixture to enable fatty acid quantification. Methylation of the fatty acids to fatty acid methyl esters (FAMEs) and the quantification of the FAMEs by GC/MS analysis were performed as described by Breuer et al. [27]. TFA concentration was calculated as the sum of triacylglycerides (TAG) and polar lipids (PL).

2.2.3 Triacylglycerides and polar lipids

Quantification of TAG was similar to the TFA analysis method with some modifications. After TFA extraction, the chloroform-methanol mixture was evaporated under N_2 gas and the TFA fraction dissolved in 1 mL hexane and separated based on polarity using a Sep-Pak Vac silica cartridge (6 cc, 1,000 mg; Waters, Milford, MA, USA) equilibrated with hexane. The neutral TAG fraction was eluted with 5 column volumes (10 mL) of hexane-diethyl ether (7:1 v/v). Subsequently the polar lipid fraction containing glycolipids and phospholipids was eluted from the silica cartridge with 5 column volumes (10mL) of methanol:acetone:hexane (2:2:1 v/v/v). All solvents were then evaporated from the fractions under N_2 gas. TAG and PL fractions were then methylated and analysed as described in the TFA analysis section.

2.2.4 Total carbohydrates

Total carbohydrates were extracted and analysed by a colorimetric assay according to DuBois et al. (1956). A biomass dry-weight of ~20 mg was hydrolysed in 5 mL 2.5 M HCl in a heat block at 100°C for 3 h. Samples were neutralized using 5 mL of 2.5 M NaOH. Then 0.5 mL of

5% w/w phenol and 2.5 mL of concentrated sulfuric acid was added to 0.5 mL of hydrolysed sample. The samples were incubated at 35°C for 30 min before reading of the absorbance at 485 nm against a blank of 0.5 mL 5% w/w phenol, 2.5 mL concentrated sulfuric acid and 0.5 mL of deionized water. Glucose was used as a standard.

2.2.5 Starch

Starch content was analysed by enzymatic degradation of starch to glucose using the thermostable α-amylase and amyloglucosidase enzymes from the Total Starch Assay Kit (AA/AMG) (Megazyme International, Ireland) using the protocol described by de Winter et al. [28]. Around 10 mg of freeze-dried cells were disrupted by bead beating in bead beating tubes (Lysing Matrix E; MP Biomedicals) in the presence of 80% ethanol. Starch was then converted to glucose using the α-amylase and amyloglucosidase enzymes from the kit. Subsequently glucose was coloured, and absorbance was measured against a D-glucose calibration control series at a wavelength of 510 nm.

2.2.6 Protein

Protein concentration was determined on 5 and 10 mg of freeze-dried cells using the Lowry DC protein assay (BioRad).

2.2.7 Biomass productivity/production rates

Biomass productivity, r_x, was computed according to equation (1). In equation 1, Δx is the biomass concentration changes in the PBR during the period Δt; $\overline{x}$ is the averaged biomass concentration (considering the initial and final biomass concentration of each period); Q_A is the media flow rate, V_R is the reactor volume; and, r_x is the actual biomass productivity.

8

$$\text{Equation (1)} \quad \frac{dx}{dt} = \frac{Q_A}{V_R}x + r_x \approx \frac{\Delta x}{\Delta t} = \frac{Q_A}{V_R}\bar{x} + r_x$$

The productivities of each metabolite were calculated from equation (1), considering their intracellular concentrations.

2.3 RNA isolation, RNA-Seq library preparation and sequencing

Total RNA was extracted from microalgal cells (~100-200 mg wet weight) by cell disruption by bead-beating in bead-beater tubes (Lysing Matrix E; MP Biomedicals, Santa Ana, CA, USA) for 1x10 sec at 5500 rpm in a Precellys® 24 bead beater (Bertin Technologies), in the presence of RLT buffer with β-mercaptoethanol (Qiagen). Subsequently, tubes were placed on ice and spun down for 2 min at 13.000 x g. RNA was further cleaned using the RNeasy Plant Mini Kit (Qiagen). In short, supernatant was transferred to a Qiashredder column, and columns centrifuged for 2 min at 13.000 x g. Supernatant was transferred to a 2 mL Eppendorf vial, 0.5V of 96% ethanol was added and mixed. The mixture was then processed on Qiagen RNeasy columns, including on-column DNaseI treatment, according to the manufacturers' instructions. Further preparation of RNA and RNA sequencing was performed by BaseClear (Leiden, The Netherlands).

RNA quality control and quantification were performed using a BioAnalyzer and an Illumina TruSeq strand-specific mRNA library was prepared (average mRNA library size of 345 bp) for the construction of the reference transcriptome using 125 bp paired-end sequencing (PE 125) from a pool of all RNA samples (N-replete and N-deplete). Individual sample libraries were prepared by 50 bp single-end read sequencing (SR 50). Paired-end and single-end sequencing reads were generated using the Illumina HiSeq2500 instrument. FASTQ sequencing files were generated using the Illumina CASAVA software and internally quality filtered based on Illumina's chastity filtering procedure, then PF reads (raw reads) were used for further analysis.

9

Time series data discussed in this publication have been deposited in NCBI's Gene Expression Omnibus [29] and are accessible through GEO Series accession number GSE104807 (https://www.ncbi.nlm.nih.gov/geo/query/acc.cgi?acc=GSE104807).

2.4 *De-novo* transcriptome assembly and functional annotation

RNA-seq raw reads were quality controlled using FASTQC v.0.11.3 and Trimmomatic [30] (automatically invoked by Trinity software [31]). The reference transcriptome was assembled with Trinity v.2.0.6 using the following parameters: --seqType fq --SS_lib_type FR --trimmomatic --quality_trimming_params SLIDINGWINDOW:20:25 MINLEN:80 and have been deposited at DDBJ/EMBL/GenBank under the accession GFXW00000000.

Trinotate v.2.0.2 (https://trinotate.github.io) was used for transcriptome annotation. Transcripts and their predicted ORFs were queried with BLASTx and BLASTp against both the SwissProt [32] and UniRef90 [33] databases and only the top-scoring hit was retained. HMMER [34] was used to search for conserved protein domains in predicted ORFs against the pfam-A database [35]. BLAST homologs and Pfam domain entries were loaded into the pre-formatted Trinotate SQLite database which contained UniProt-associated annotation information. The subcellular localizations of each protein were predicted using a standalone version of TargetP v1.1 [36] in plant mode and without cut-offs (winner takes it all).

2.5 Transcript abundance and differential expression analysis

Scripts bundled with Trinity software were mainly adopted to quantify the transcripts and find the differentially expressed subset. Transcript-level rather than unigene-level expression was investigated to retain isoform-specific information. Reads from individual libraries were aligned to the reference transcriptome with bowtie v.1.1.2 [37] and quantified using RSEM v.1.2.19 [38]. A table of TMM-normalized FPKM expression matrix and a separate table of

raw fragment counts were generated for further analysis and visualization. Differentially expressed (DE) transcripts were identified from raw counts with the Bioconductor package EdgeR v.3.1 [39]. Three biological replicates for each condition were provided. The most significant differentially expressed transcripts (FDR<0.001 and FC>4) were extracted for further analysis. A hierarchically clustered heatmap was generated from the Pearson correlation matrix of pairwise sample comparisons based on the most significant DE subset. The most significant DE subset was also partitioned into expression clusters by cutting hierarchical clustering trees of transcripts using MeV v.4.9.0 (https://sourceforge.net/projects/mev-tm4/).

2.6 Gene ontology analysis

GO terms were extracted from transcriptome annotation using scripts from Trinotate and visualized using BGI's WEGO [40]. GO functional enrichment tests on differentially expressed transcripts were performed with scripts from Trinity v2.4.0 that wrapped the Bioconductor package GOseq [41]. Blast2GO v.4.0.7 [42] was used to map GO terms to plant GO Slim [43] terms in order to obtain a broad overview of the transcriptome. For each time point, enriched GO terms were visualized using GOplot v1.0.2 [44]. Most significant over- and under-represented GO terms (top 10 for each time point, then combined) were extracted using custom scripts and visualized using the GOplot package (http://wencke.github.io/).

2.7 KEGG pathway analysis

A standalone version of KOBAS 2.1.0 [45] was used to functional annotate the transcriptome with KO terms, the corresponding pathways and enzymes were extracted from information retrieved using KEGG API. The TMM-normalized FPKM expression matrix was filtered by removing low expressed transcripts (average expression value below 1) and transcripts without proper KO terms, then used as input for Pathview ([46]; online version) to visualize significant

650
651
652
653
654
655
656
657
658
659
660
661
662
663
664
665
666
667
668
669
670
671
672
673
674
675
676
677
678
679
680
681
682
683
684
685
686
687
688
689
690
691
692
693
694
695
696
697
698
699
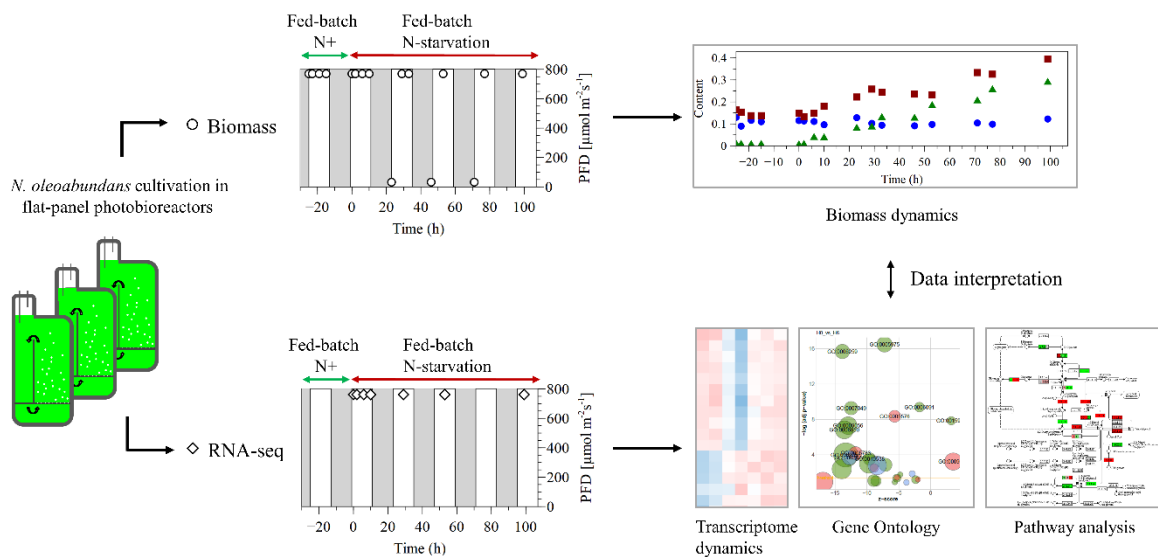700
701
702
703
704
705
706
707
708

pathways (internally use GAGE [47] for pathway enrichment analysis) and some manually selected pathways. Pathways with q-values smaller than 0.05 were combined and shown as heatmaps.

3. Results

N. oleoabundans was grown in fed-batch mode in controlled flat-panel photobioreactors and subjected to full nitrogen-starvation during a 4-day period. Before and during this starvation period, culture parameters were monitored and physiological and transcriptional changes in culture samples measured to determine the temporal dynamics of the nitrogen-stress response. For the fed-batch pre-cultures grown in nitrogen-replete conditions (+N) samples were taken at four timepoints in the light-phase preceding nitrogen starvation, while from the onset of nitrogen starvation (-N), time-series samples were taken at the start, middle and end of the light-phase and at the end of the dark-phase over a 4-day period (Fig. 1).

Fig. 1. Experimental design for analysis of the temporal dynamics of cellular content, storage compound accumulation and transcriptional response in nitrogen-replete (N+) and nitrogen-starvation (N-) conditions in *N. oleoabundans*. Nitrogen starvation was initiated at t=0 hrs. *N. oleoabundans* was

cultivated in triplicate in flat-panel air-lift photobioreactors at a photon flux density (PFD) of 800 µmol m^{-2} s^{-1} and a 12:12 day-night cycle. Alternating 12 hrs light phases (white background) and 12 hrs dark phases (grey background) are indicated. Individual sampling time points for biomass analysis (open circles) and RNA-seq analysis (open diamonds) are depicted, and were taken in the light phase (marker at top of light phase) or in the dark phase (marker at bottom of dark phase).

3.1 Biomass dynamics under nitrogen starvation

Upon nitrogen starvation, *N. oleoabundans* could sustain an increase in biomass concentration (cell dry weight) during the light phase in the first two days (Fig. 2A). Overall, the biomass concentration gradually decreased, which coincided with a decreased biomass productivity over time (Fig. 2D). The protein content and quantum yield (QY) also showed a steady decline throughout the starvation period (Fig. 2D and Supplementary Fig. A.1).

Nitrogen starvation induced the fast accumulation of carbohydrates, increasing from 15% at the start to a maximum content of 33% of the cell dry weight after 10 hrs starvation. Within the same time frame and with the same accumulation pattern, starch content increased from 8% at the start to a maximum content of 28% of the cell dry weight (Fig. 2B). This indicated that the increase in total carbohydrates was mainly due to starch accumulation. The starch content subsequently decreased again to N-replete levels of 18% in the light phase at day 4. During the dark phases starch was consumed and decreased to 15% content then. In contrast, accumulation of total fatty acids (TFA) was more gradual from a content of 16% at the start to a maximum of 41% after 4 days. A decrease of fatty acids in the dark phases, indicating fatty acid consumption, was not observed. The increase in lipid content was mainly due to TAG accumulation, which increased from a content of 0.4% to 30% after 4 days, while the polar lipid (PL) content was stable around 10-13% (Fig. 2C). This indicates that TAG biosynthesis occurred mainly *de novo,* although some interconversion from starch to TAG or from membrane lipids to TAG cannot be excluded.

13

768
769
770
771
772
773
774
775
776
777
778
779
780
781
782
783
784
785
786
787
788
789
790
791
792
793
794
795
796
797
798
799
800
801
802
803
804
805
806
807
808
809
810
811
812
813
814
815
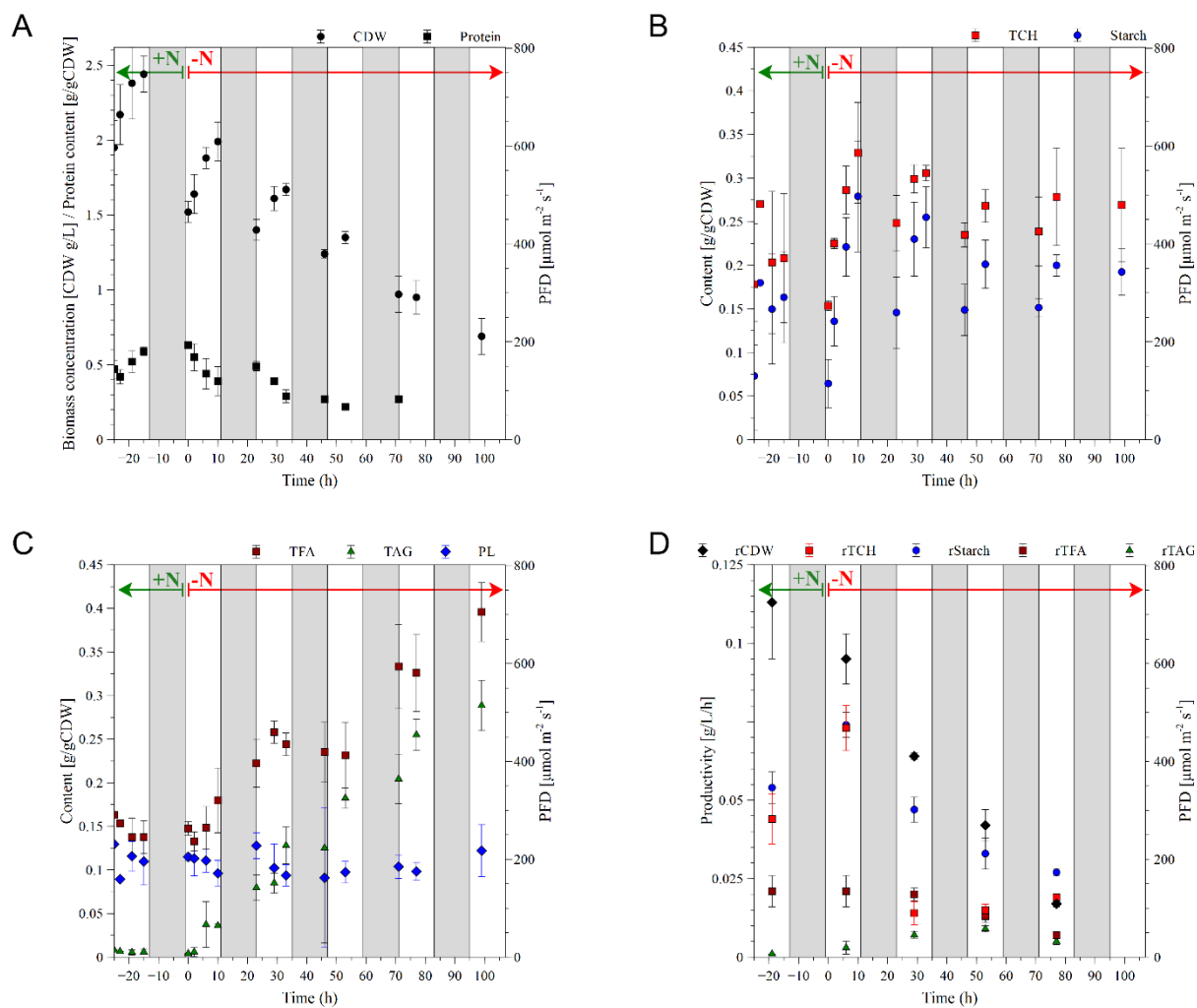816
817
818
819
820
821
822
823
824
825
826

Fig. 2. Dynamics of cellular content in *N. oleoabundans* grown in N-replete (+N) and N-starvation (-N) conditions in air-lift flat-panel photobioreactor. (A) Biomass concentration [CDW g/L] and protein content [g/gCDW]. (B) Total carbohydrates (TCH) and starch content (% of CDW). (C) Total fatty acids (TFA), triacylglycerides (TAG) and polar lipids (PL) content (% of CDW). (D) Productivities of biomass (rCDW), total carbohydrates (rTCH), starch (rStarch), total fatty acids (rTFA) and triacylglycerides (rTAG). Results are shown as mean values ± standard deviations (n=3). The onset of N-starvation is at t=0 hrs. The 12:12 day-night cycles used for cultivation are shown as alternating 12 hrs light phases (white background) and 12 hrs dark phases (grey background).

Concomitant with the accumulation of storage compounds the fatty acid composition of the different lipid fractions also changed during nitrogen starvation. A clear change from polyunsaturated fatty acids (PUFAs) towards mono-unsaturated and saturated fatty acids was

14

observed in all fractions (Fig. 3). Under N-replete conditions a large part of all lipid fractions was composed of C18:3 and C16:3 fatty acids (approximately 30% and 15%, respectively). These species decreased during N-starvation (to 5% and 2.5%, respectively), while there was an increase in the (mono-)unsaturated fatty acids C18:1, C16:2 and C16:1 and the saturated fatty acid C18:0 respectively. The biggest change was observed for C18:1 that increased from 5% to almost 40% in the lipid fraction.

Production rates for total carbohydrates (TCH) and starch showed an identical rapid increase during the first day of N-starvation. This indicates that increased TCH levels in the first day can mainly be ascribed to starch production. Subsequently, both TCH and starch production rates decreased to levels below those for N-replete growth, although more severe for TCH. This means that production rates of carbohydrates other than starch were reduced much stronger. In the lipid fraction TAG productivity increased slowly in the first 2 days following N-starvation, and then decreased again to N-replete rates. The total lipid productivity remained stable on the first day of N-starvation and then started to decrease (Fig. 2D).

886
887
888
889
890
891
892
893
894
895
896
897
898
899
900
901
902
903
904
905
906
907
908
909
910
911
912
913
914
915
916
917
918
919
920
921
922
923
924
925
926
927
928
929
930
931
932
933
934
935
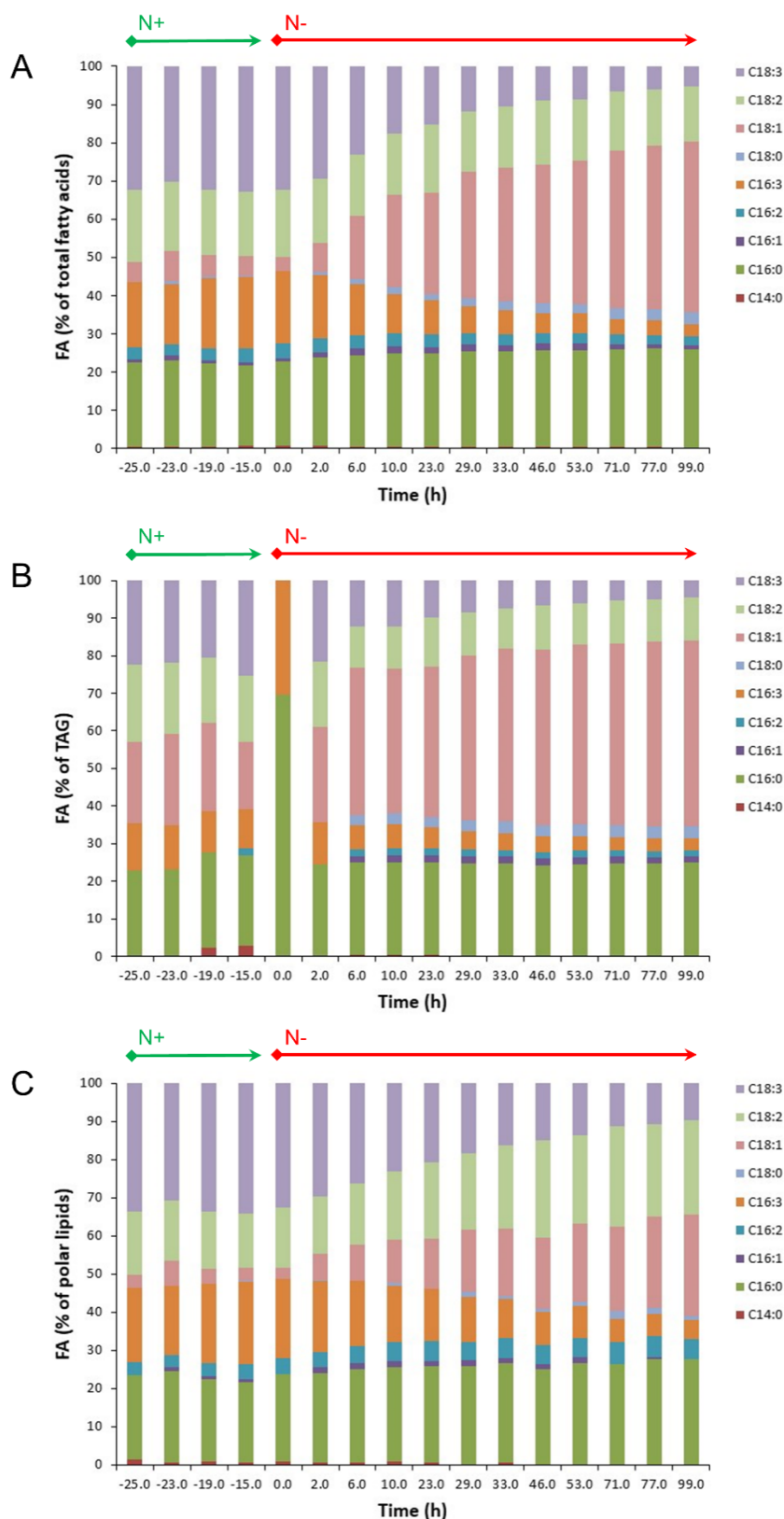936
937
938
939
940
941
942
943
944

Fig. 3. Fatty acid composition of (A) total fatty acids, (B) TAG and (C) polar lipids fractions of *N. oleoabundans* grown in N-replete (N+) and N-starvation (N-) conditions in air-lift flat-panel photobioreactors. Mean values (n=3) are shown. Onset of N-starvation is at t=0 hrs.

3.2 Differential gene expression dynamics under nitrogen starvation

A total of 25.6 million high-quality RNA-seq clean reads were *de novo* assembled into 61,010 transcripts belonging to 42,338 'genes' with a N50 length of 1,838 bp and average GC content of 58.9% (Table 1). Functional annotation of the transcriptome was carried out with the Trinotate pipeline, and 44,789 transcripts (73.4%) were annotated using UniRef90 database (Table 1). The high-quality reference transcriptome served as a solid foundation for subsequent gene expression analysis.

Table 1. Summary of *de novo* transcriptome assembly and annotation for *N. oleoabundans*.

Features		Results
Reads	Raw reads	27.19 M
	Clean reads	25.58 M
Assembly	Number of transcripts	61,010
	Transcriptome size (Mbp)	70.8
	Mean (bp)	1,161
	Median (bp)	800
	N50 length (bp)	1,838
	GC (%)	58.9
Annotation	Swiss-Prot	27,765 (45.5%)
	UniRef90	44,789 (73.4%)
	GO	21,591 (35.4%)
	KO	15,336 (25.1%)

3.2.1 Global gene expression analysis

Time series experiments were performed (7 time-points, 3 replicates; GEO accession GSE104807), reads from each RNA-seq library were individually aligned back to the reference transcriptome and the abundance of each transcript was determined. The hierarchical clustering of transcripts from samples obtained from triplicate photobioreactors indicated a good experimental reproducibility (Supplementary Fig. A.2). Differentially expressed transcripts were then determined from raw count values for each time point from the onset of N-starvation. A total of 12,975 transcripts were either up-regulated or down-regulated compared to control

17

samples (0h) and the number varied between different time points (2,014~6,589) (Supplementary Table 1).

Hierarchical clustering of expression profiles of each transcript resulted in 23 distinct expression clusters (Fig. 4 and Supplementary Table 1). The largest clusters were cluster 21, 15, 11 and 4, which contained 2938, 1834, 1145 and 1081 differentially expressed gene isoforms respectively. Many transcripts related to fatty acid, TAG and starch metabolism belong to these clusters. The diverse expression clusters to which the genes from a metabolic route belong to, indicates that different genes from these metabolic pathways are most probably under the control of different transcriptional regulators and therefore do not follow simultaneous activation. Some transcriptional regulators group into these clusters as well and might play a regulatory role in the nitrogen-starvation activated response of fatty acid and starch biosynthesis genes. These include transcriptional regulators such as the 5'-AMP-activated and SNF1-related protein kinases (TR3188|c0_g1 and_g2, and TR24203|c0_g1), a dual specificity tyrosine-phosphorylation-regulated kinase (DYRK3: TR935|c0_g2_i1), PHR1-LIKE 1 protein (PHL1: TR19823|c0_g1) and a nitrogen regulatory protein P-II homolog (GLNB: TR228|c0_g1 and TR228|c0_g3). Clusters 1-3, 12, 19 and 20 showed very distinct expression peaks and interestingly several transcripts related to reactive oxygen stress grouped to the clusters 12, 19 and 20. Detailed description of the transcriptional response to nitrogen starvation is discussed below.
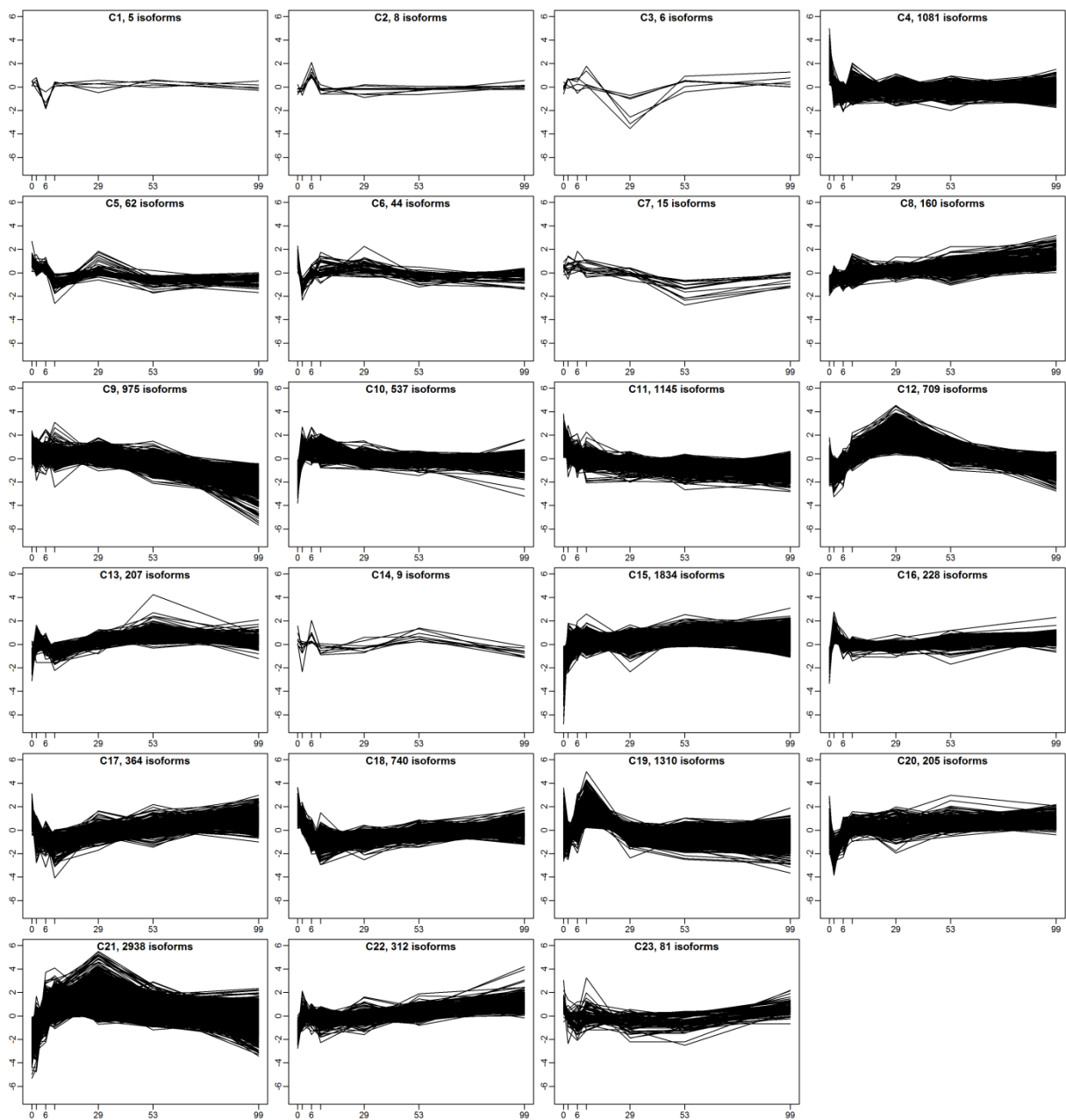
Fig. 4. Hierarchical clusters of gene expression profiles during nitrogen starvation. Expression levels are shown as median-centered log2(fpkm+1) values for the time series H0-H99 and the number of transcript isoforms in each cluster are indicated.

The GO terms for upregulated transcripts were enriched with terms related to fatty acid and lipid metabolism as well as carbohydrate and starch metabolism, as is expected in view of the observed biomass changes (Supplementary Fig. 4 and Supplementary Table 2). In addition, GO terms for ammonium uptake and incorporation were enriched (direct response to absence of nitrogen) as well as GO terms related to reactive oxygen species (ROS) stress, indicating that N-starvation might cause the production of ROS. The GO terms for downregulated transcripts were enriched with terms related to the chloroplast and photosynthesis, which makes sense in view of the breakdown of pigments (cell bleaching) and reduced photosynthetic capacity (e.g. quantum yield) due to the lack of nitrogen (Supplementary Fig. A.4 and Supplementary Table 3). Taken together, GO analysis indicates that most of the transcripts can be grouped into a small number of broad yet distinct functional categories that correlate well to the observed biomass and physiological changes. GOBubble plots based on plant GO Slim terms (Supplementary Fig. A.4) showed that the highest number of increased and decreased GO Slim terms was found after 6 to 10 hrs of nitrogen starvation. This indicates that most transcriptional changes upon nitrogen starvation occur relatively rapid. The broader GO Slim terms indicated that "carbohydrate metabolic process" (GO:0005975) was the only GO Slim term that for all time points significantly increased compared to T=0 (negative z-score H0 versus other time points). Other GO Slim terms like "catabolic process" (GO:0009056) and "response to stress" (GO:0006950) also increased for an extended period. In contrast, the GO Slim terms for "photosynthesis" (GO:0015979), "plastid" (GO:0009536) and "thylakoid" (GO:0009579) were clearly decreased from 6 to 29 hrs (positive z-score H0 versus other time points), indicating a reduction in the photosynthetic capacity.

KEGG pathway enrichment was performed using GAGE (Supplementary Table 4) and data were mapped on KEGG pathways to generate graphs showing detailed temporal changes (Supplementary Fig. A.5). The most striking observations from the KEGG pathway enrichment

analysis was an up-regulation of the TCA cycle (ko00020), Proteasome (ko03050), Protein processing in endoplasmic reticulum (ko04141) and Phagosome (ko04145) pathways, and a down-regulation of the Photosynthesis (ko00195) pathway (Supplementary Table 4). This indicates increased protein and organelle degradation and correlates with the increased GO Slim terms such as "catabolic process" (GO:0009056), "generation of precursor metabolites and energy" (GO:0006091) and "protein metabolic process" (GO:0019538), as well as the decreased photosynthesis, plastid and thylakoid GO Slim terms mentioned above (Supplementary Fig. A.4) and decrease in quantum yield (Supplementary Fig. A.1).

3.2.2 Transcriptional changes in starch metabolism

The transient and rapid increase in starch productivity and accumulation in the first 10 hrs of N-starvation coincided with increased expression of several genes involved in starch biosynthesis (Fig. 5 and Supplementary Table 1). In particular, starch biosynthesis genes encoding phosphoglucomutase (conversion of glucose-6-phosphate to glucose-1-phosphate) showed a strong up-regulation in expression from the onset of N-starvation, while the ADP-glucose phosphorylase (conversion of glucose-1-phosphate to ADP-glucose) was only up-regulated from 10 hrs on. Multiple starch synthase genes showed different responses. While the soluble starch synthase SSY3 and the granule-bound starch synthases SSG1 and SSG2 showed a fast and transient up-regulation from 2 to 6 hrs from the start, the soluble starch synthase SSY2 showed a strong transient increase in expression from 6 to 10 hrs. Likewise, the 1,4-alpha-glucan-branching enzyme (GLGB1) that modifies amylose to starch was only up-regulated in the first 6 hrs. Among the starch degradation genes, gene expression of the alpha-glucan water dikinase (GWD1) was increased from 6 hrs on. This enzyme increases the phosphorylation-level of starch and thereby stimulates the degradation of starch in higher plants and *Chlamydomonas* [48]. Starch breakdown involves several amylases and we found that

21

multiple genes for α-amylase (AMY1 and AMY3), β-amylase (AMYB, AM1, BAM1) and isoamylase (ISOA1 and ISOA3) showed fluctuating expression responses. Overall though, they exhibited down-regulation at the start of starch accumulation and up-regulation in the later stages, from 6 to 10 hrs on. Hexokinase performs the first step in glycolysis, the conversion of glucose to glucose-6-phosphate, and hexokinase genes were upregulated from 10 hrs starvation on. This indicates breakdown of glucose, which for a large part could be starch-derived glucose, as starch degradation increases from this time on as well. Overall, these results suggest that the increased production and accumulation of starch can mainly be attributed to the strong up-regulation of the starch biosynthesis genes and less to a decrease in starch degradation. The subsequent decrease in starch productivity and accumulation from 29 hrs on concurred with decreased gene expression for the soluble starch synthase SSY2 as well, which supports this hypothesis.
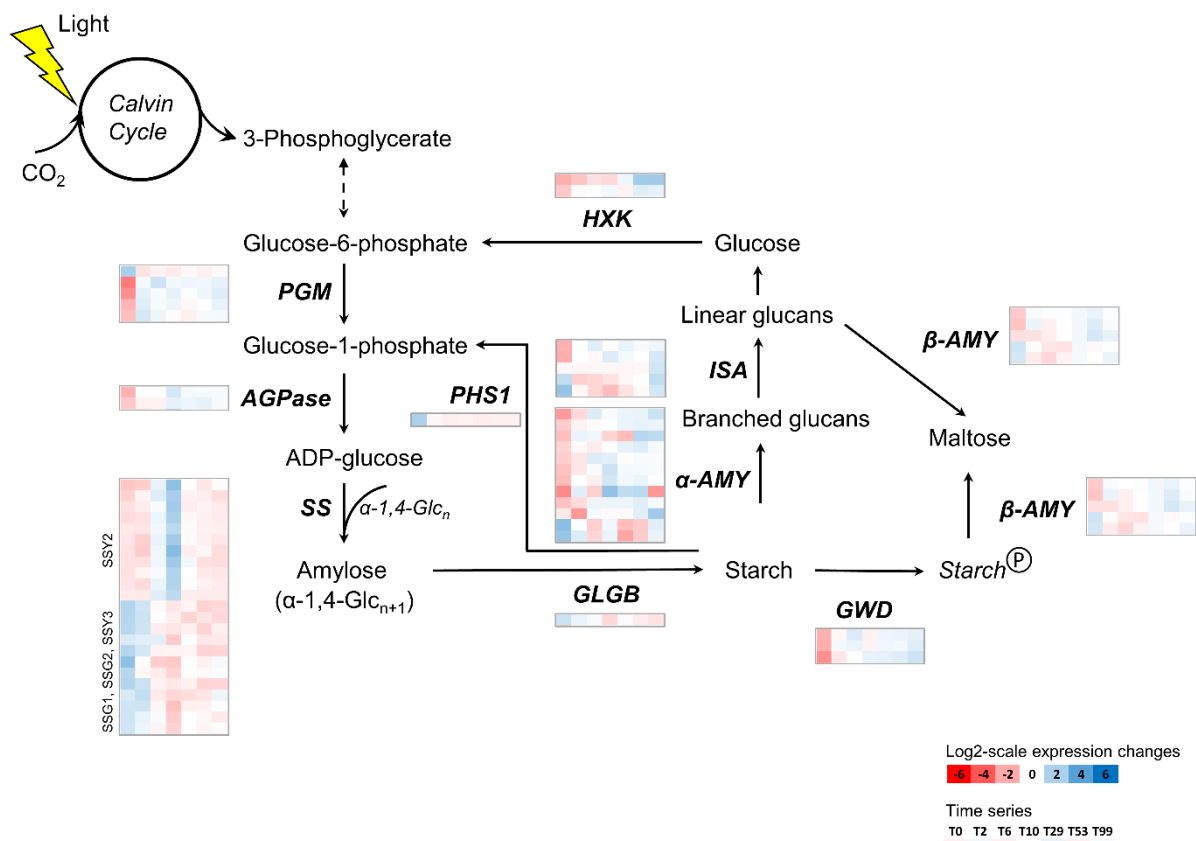
Fig. 5. Differential expression of starch biosynthesis genes during nitrogen starvation. Heatmaps of expression levels per transcript are shown as median-centered log2(fpkm+1) values sequentially for time series T0-T99. The inset shows the log2 colour coding scale. PGM, phosphoglucomutase; AGPase, ADP-glucose phosphorylase; SS, starch synthases; HXK, hexokinase; PHS1, alpha-glucan phosphorylase; GLGB, 1,4-alpha-glucan-branching enzyme; ISA, isoamylase; α-AMY, alpha-amylase; β-AMY, beta-amylase; GWD, alpha-glucan water dikinase; α-1,4-Glc, alpha-1,4-glucan. Starch^P indicates starch targeted for degradation through increased phosphorylation by GWD.

3.2.3 Transcriptional changes in fatty acid and lipid metabolism

Transcriptional changes for genes related to lipid biosynthesis (Fig. 6 and Supplementary Table 1) also correlated with the observed increase in productivity and accumulation of TFA and TAG (Fig. 2). Several genes required for fatty acid biosynthesis showed increased expression within 2 to 10 hrs from N-starvation. The first step in fatty acid biosynthesis requires the precursor acetyl-CoA, which can be derived from different biochemical conversions. A first route is via the pyruvate dehydrogenase complex (PDH) that converts pyruvate to acetyl-CoA. A second route is via acetyl-CoA synthetase (ACS), that converts acetate to acetyl-CoA. Finally, a third route is via the TCA cycle where ATP citrate lyase (ACLY) can convert citrate to acetyl-CoA and oxaloacetate. Gene expression of the PDH subunits ODPA1 and ODPB1 (TR1574|c0_g2 and TR13897|c0_g2), several acetyl-CoA synthetases (TR16088|c0_g1/g2, TR18695|c0_g1, TR2994|c0_g1/g2/g3 and TR26776|c0_g1) and ATP citrate lyases (TR25574|c0_g2 and TR26430|c0_g2) clearly increased within 2 to 10 hrs from N-starvation and remained so until 99 hrs of starvation. Increased expression of PDH, ACS and ACLY genes can result in a higher supply of acetyl-CoA, the precursor for fatty acid biosynthesis, and thereby increase the carbon-flux towards lipid synthesis (Fig. 6). The subsequent steps in fatty acid biosynthesis involve acetyl-CoA carboxylase (ACCase) and malonyl-CoA-ACP transacylase (FABD), and gene expression for these enzymes also increased in the first 10 hrs from N-starvation. The fatty acid

23

synthesis (FAS) complex genes were up-regulated as well, including the ones encoding chloroplastic 3-oxoacyl-ACP synthase I (KASC1), 3-oxoacyl-ACP reductase (FABG), NADPH-dependent enoyl-ACP reductase (FABL) and 3-hydroxyacyl-ACP dehydratase (FABZ), as well as the acyl-ACP thioesterase (FATA). Overall however, this response was more delayed than that for starch biosynthesis.

For subsequent biosynthesis of triacylglycerides (TAG), transcripts encoding glycerol kinase (GK), glycerol-3-phosphate dehydrogenase (GPDA), two glycerol-3-phosphate O-acyltransferases (GPAT) and the phosphatidic acid phosphatase (PAP) were strongly up-regulated from 2 hrs after the onset of N-starvation, while gene expression of lyso-phosphatidic acid acyltransferase (LPAT) - which is responsible for the intermediate conversion of lysophosphatidic acid to phosphatidic acid - only increased from 29 hrs on. These genes perform biosynthesis of the lipid backbone glycerol-3-phosphate (G3P) and the subsequent incorporation of free fatty acids up to diacylglycerol (DAG). The diacylglycerol O-acyltransferases (DGAT) genes required for the final conversion of diacylglycerol (DAG) to triacylglycerol (TAG) also showed an initial decrease in expression, but were clearly up-regulated only from 29 hrs of N-starvation on, indicating that the DAG pool is built up before the final DAG to TAG conversion. Both a DGAT-1 and a DGAT-2 gene were up-regulated and appear to be responsible for the final conversion of DAG to TAG. The transcriptome annotation predicted a single DGAT-1 gene and five DGAT-2 gene sequences, and our data indicate that only one of the five DGAT-2 genes responds to N-starvation. The subcellular locations of these DGAT enzymes and the corresponding TAG biosynthesis pathways in *N. oleoabundans* are still to be determined. Interestingly, a gene encoding a putative lipid body-associated caleosin (peroxygenase) protein (TR11980|c0_g1_i1) was also up-regulated from 29 hrs on, indicating that increased lipid body formation is concomitant with DAG to TAG biosynthesis. Incorporation of free long-chain fatty acids into lipids requires the activation to their acyl-CoA

24

form, which is usually performed by long-chain acyl-CoA synthetases (LACS). A gene isoform encoding a chloroplastic long-chain-fatty-acid CoA ligase (TR19322|c0_g1_i1) showed up-regulation from 53 hrs on and might serve this role.
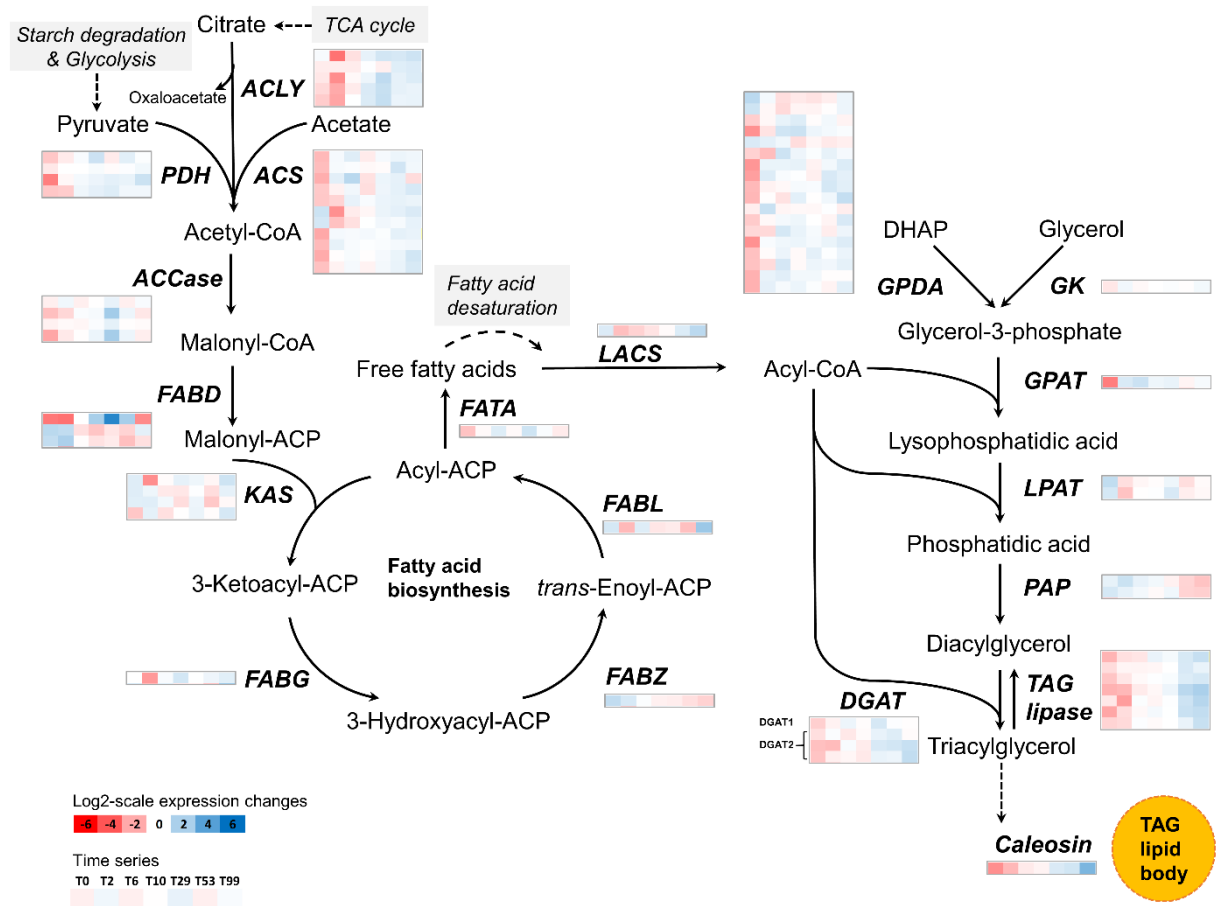

Fig. 6. Differential expression of fatty acid and triacylglyceride biosynthesis genes during nitrogen starvation. Heatmaps of expression levels per transcript are shown as median-centered log2(fpkm+1) values for the time series T0-T99. The inset shows the log2 colour coding scale. PDH, pyruvate dehydrogenase complex; ACS, acetyl-CoA synthase; ACCase, acetyl-CoA carboxylase; FABD, malonyl-CoA-ACP transacylase; KAS, 3-oxoacyl-ACP synthase; FABG, 3-oxoacyl-ACP reductase; FabZ, 3-hydroxyacyl-ACP dehydratase; FABL, NADPH-dependent enoyl-ACP reductase; FATA, acyl-ACP thioesterase; LACS, long-chain acyl-CoA synthetase, G3PDH, glycerol-3-phosphate dehydrogenase; GK, glycerol kinase; GPAT, glycerol-3-phosphate O-acyltransferases; LPAT, lyso-phosphatidic acid acyltransferase; PAP, phosphatidic acid phosphatase; DGAT, diacylglycerol O-acyltransferase; TAG lipase: triacylglyceride lipase.

25

TAG lipase activity negatively affects TAG accumulation, while phospholipases are involved in liberation of free fatty acids from (plastid) membrane lipids and interconversion into TAG. Transcript levels of two TAG lipase genes (SDP1: TR9756|c0_g3 and TR22634|c0_g2_i1) were decreased in the first 10 hrs of N-starvation, while at the end of N-starvation a marked increase was observed (Supplementary Table 1). The late upregulation of TAG lipases follows the earlier up-regulation of TAG biosynthesis genes, which could explain the initial steady increase in TAG accumulation and final levelling-off in TAG productivity. Besides *de novo* TAG synthesis, interconversion from membrane lipids to TAG is a common mechanism under stress conditions in microalgae [49–52], and the enzyme phospholipid:diacylglycerol acyltransferase (PDAT) plays an important role in this [51,53]. A PDAT homolog was not identified in our reference transcriptome, but several chloroplastic phospholipase A1 genes (DAD1 homologs) did show increased expression at different timepoints during N-starvation (Supplementary Table 1). Phospholipase activity results in the conversion of phospholipids to lysophospholipids and free fatty acids. Lysophospholipase subsequently converts lysophospholipids further to free fatty acids and glycerol-phosphate derivates [54,55]. A lysophospholipase gene (TR21369|c0_g1_i5) showed increased expression from 29 hrs on. Reacylation of lysophospholipids to phospholipids is performed by lysophospholipid transferases, and two lysophospholipid transferase genes (LPT1: TR19784 and TR9894|c0_g2_i1) were down-regulated within the first 10 hrs. The gene expression profiles of the (lyso)phospholipases and lysophospholipid transferases could indicate that free fatty acids are liberated from membrane phospholipids upon nitrogen starvation, which subsequently can be used in TAG biosynthesis. The decrease in chloroplast-related GO Slim terms in the period before the clear increase in DGAT expression at 29 hrs also supports that TAG biosynthesis initially was not only *de novo*, but might also be the result of some interconversion from membrane lipids to TAG. Altogether, there are several indications that in the earlier stages of N-starvation there is active recycling of

26

plastidial membrane phospholipids taking place, therefore incorporation of membrane-derived fatty acids into TAG cannot be excluded and awaits further investigation, e.g. by using carbon radiolabelling studies. Expression of a chloroplastic monogalactosyldiacylglycerol synthase gene (MGDGS: TR23849|c0_g1_i) was down-regulated from 6-53 hrs (Supplementary Table 1). MGDG synthase couples UDP-galactose and DAG to form the galactoglycerolipid monogalactosyldiacylglycerol (MGDG) which is abundantly present in the photosynthetic membranes of chloroplasts in higher plants and microalgae [56–58]. It thereby competes with DGAT enzymes for the chloroplastic DAG pool and decreased expression of MGDG synthase indicates reduced production of chloroplast-MGDG, leaving more DAG available for TAG synthesis. Finally, gene expression of chloroplast lipid transporters (TRIGALACTOSYLDIACYLGLYCEROL TGD1 and 2: TR2378|c0_g1_i1 and TR29717) was up-regulated. TGD proteins are present in the chloroplast membrane in *Chlamydomonas*, and facilitate the transport of lipids derived from the endoplasmic reticulum (ER) into the chloroplast [58]. Up-regulation of these genes under nitrogen starvation in *N. oleoabundans* could indicate that in this way starved cells try to compensate for the decrease in chloroplast lipids as we hypothesize above.

Expression of several chloroplast-specific fatty acid desaturase (FAD) genes was repressed from 6 hrs on (Fig. 7), which explains the increased incorporation of mono-unsaturated (C18:1 and C16:1) and saturated (C18:0) fatty acids in the different lipid fractions and decrease of C18:3 and C16:3 fatty acids. The combined reduction in expression of FAD6C (C16:1 → C16:2 and C18:1 → C18:2) and FAD3C (C16:2 → C16:3 and C18:2 → C18:3) supports the increase in the C16:1, C16:2 and C18:1 fatty acid fractions. Concomitant with this, expression of the elongase-complex genes 3-ketoacyl-CoA synthase (KSC1), very-long-chain (3R)-3-hydroxyacyl-CoA dehydratase (HACD) and very-long-chain enoyl-CoA reductase (ECR) showed increased expression. This could result in higher C16:0 to C18:0 conversion, and higher

27

1594
1595
1596
1597
1598
1599
1600
1601
1602
1603
1604
1605
1606
1607
1608
1609
1610
1611
1612
1613
1614
1615
1616
1617
1618
1619
1620
1621
1622
1623
1624
1625
1626
1627
1628
1629
1630
1631
1632
1633
1634
1635
1636
1637
1638
1639
1640
1641
1642
1643
1644
1645
1646
1647
1648
1649
1650
1651
1652

C18:0 levels could thereby increase C18:1 production as well. Both increased C18:0 and C18:1 levels were observed, though C16:0 levels were not clearly reduced. This indicates that most probably the observed increase in C18:1 and C18:0 is mainly caused by the reduction in fatty acid desaturases gene expression. In support of this we did not observe significant differential gene expression of two stearoyl-ACP desaturase genes (SAD3 and SAD5) in our reference transcriptome, which are responsible for desaturation of C16:0 and C18:0. From the start of N-starvation a chloroplastic FAD4 desaturase gene expression was also reduced (TR22593|c0_g2_i1), which converts [sn-2-C16:0]-containing glycerophospholipids into [sn2-C16:1]-containing glycerophospholipids, while at the same time expression of a chloroplastic palmitoyl-monogalactosyldiacylglycerol delta-7 desaturase (ADS3, TR16760|c0_g1_i1) was upregulated in the early phases of N-starvation. This indicates decreased C16:0 to C16:1 conversion in the glycerophospholipid fraction, while in the glycolipid fraction (specifically MGDG) there was an initial increased conversion of C16:0 to C16:1. Overall, the combined effect of changes in expression of several desaturase genes involved in C16:0 to C16:1 conversion, led to an increased C16:1 content in the lipid fractions. Finally, expression of a palmitoyl-protein thioesterase gene (TR646|c0_g3_i1) was upregulated in the late stages of N-starvation. This could supply additional free palmitate (C18:0) derived from lipid-containing proteins for incorporation into e.g. TAG.
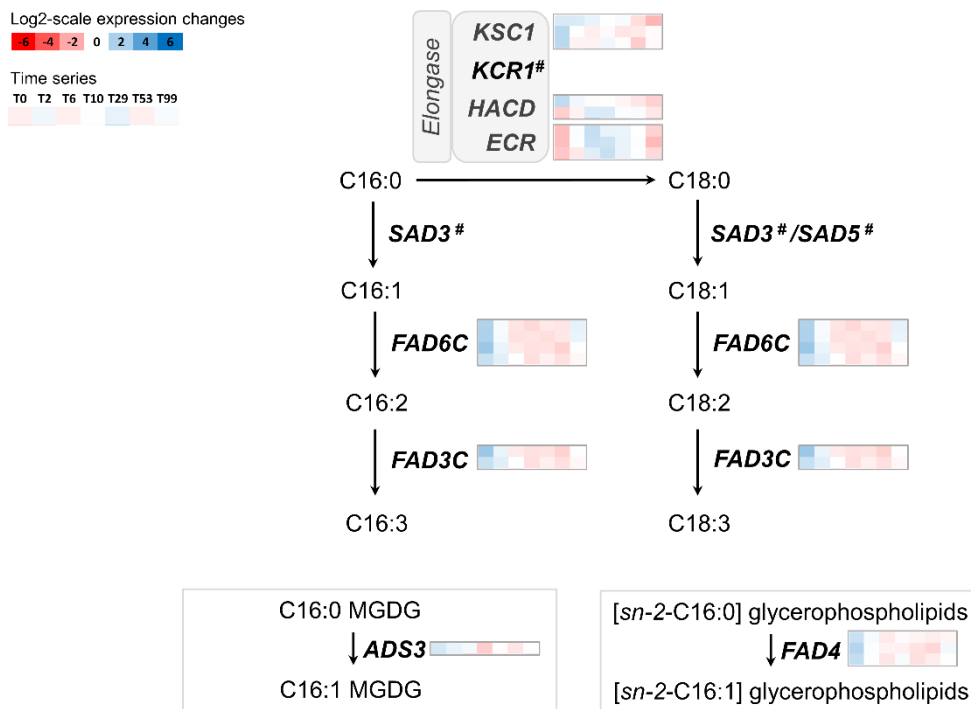
28

Fig. 7. Differential expression of fatty acid desaturase genes during nitrogen starvation. Heatmaps of expression levels per transcript are shown as median-centered log2(fpkm+1) values for the time series T0-T99. The inset shows the log2 colour coding scale. KSC1, 3-ketoacyl-CoA synthase; KCR1, (very long-chain) 3-ketoacyl-CoA reductase; HACD, very-long-chain (3R)-3-hydroxyacyl-CoA dehydratase; ECR, very-long-chain enoyl-CoA reductase; SAD, stearoyl-ACP desaturase; FAD, fatty acid desaturase; ADS3, palmitoyl-monogalactosyldiacylglycerol delta-7 desaturase; MGDG, monogalactosyldiacylglycerol. [#] No significant differential gene expression was observed.

3.2.4 Transcriptional changes in photosynthesis, carbon fixation and oxidative stress

Expression of genes for the photosystems proteins initially increased (chlorophyll a/b binding proteins), which coincided with a decreased expression of chlorophyllase (Supplementary Table 1). This could indicate that as N-starved cells cannot synthesize novel (N-containing) photosystems due to the lack of nitrogen, cells try to maintain the level of active photosystems by reducing chlorophyll degradation and maintaining its incorporation chlorophyll into existing photosystem proteins. However, at 10 to 29h post-starvation this can no longer be sustained,

indicating a decrease in photosystem biosynthesis and (most probably) photosynthetic efficiency (as can also be observed from the decreased quantum yield). The observed decrease of chloroplast-related GO Slim terms in this period is in concordance with this.

Many genes involved in CO_2 fixation (RuBisCo, PGK, PEP carboxylase, PEPC kinase) and CO_2 concentrating mechanisms (carbonic anhydrases) show a rapid up-regulation in expression in the first 2 hrs, a decrease afterwards and increase again after 99 hrs (Supplementary Table 1). This correlates to the initial sustained expression of photosystem genes and indicates that N-starved cells initially try to maintain photosynthesis and carbon fixation. Ultimately, when because of N-starvation cells cannot maintain active photosystems they can experience oxidative stress by the production of reactive oxygen species (ROS) such as hydrogen peroxide (H_2O_2) and superoxide ($O_2^{\bullet-}$) that can cause cell damage, as has been observed in e.g. *Chlorella* and *Acutodesmus* species [59–62]. In response to N-starvation, *N. oleoabundans* showed increased transcript abundance for superoxide dismutase (SOD), catalase, peroxiredoxin and several peroxidases which indicates that these ROS were produced in this species as well (Supplementary Table 1).

3.2.5 Transcriptional changes in nitrogen uptake and incorporation

As expected, N-starvation induced changes in expression of genes involved in nitrogen metabolism. The depletion of nitrate led to reduced gene expression for nitrate transporters, nitrate reductase and ferredoxin-nitrite reductase. At the same time, increased expression started for ammonium transporter genes and the glutamine synthetase (GS) and NADH-dependent glutamate synthase (GOGAT) pathways. This indicates that cells switch to an alternative mode of nitrogen incorporation via ammonium uptake (Supplementary Table 1).

3.3 Transcriptional regulators of starch and lipid accumulation

The patterns in starch and lipid accumulation suggest the existence of a regulatory mechanism for redirecting carbon-partitioning (switching) between the associated metabolic pathways. Identification of the associated "switch" regulators would be of great interest to improve existing metabolic engineering strategies that currently are often based on increased expression of a specific metabolic gene or pathway, or introduction of heterologous transcription regulators from higher plants [6].

In this study, we identified several transcriptional regulators with significantly altered gene expression upon N-starvation, some of which have been implicated in the nitrogen-starvation triggered lipid accumulation in microalgae (Supplementary Table 1). Genes encoding 5'-AMP-activated and SNF1-related protein kinases (TR3188|c0_g1 and g2, and TR24203|c0_g1, respectively) clearly showed increased expression from 10 hrs N-starvation on, and very strongly from 53h on. This is in line with a previous transcriptome study in *N. oleoabundans* [17] where after 11d of N-starvation the 5'-AMP-activated protein kinase SnRK1 showed up-regulation. SnRK1 is a global regulator of carbon metabolism in plants [63,64].

In *Nannochloropsis,* bZIP-type regulators have been implied to control several steps in the synthesis of TAG [23]. We identified two such bZIP regulators with opposite expression profiles in our transcriptome set: TR2010|c0_g1 and TR14421|c0_g1. TR14421|c0_g1 expression was activated 2 hrs after N-starvation, but showed down-regulation from 29 hrs on, while TR2010|c0_g1 was down-regulated until 53 hrs, after which the gene was activated. We also identified a transcript (TR935|c0_g2_i1) with homology to the dual specificity tyrosine-phosphorylation-regulated kinase (DYRKP) from *Chlamydomonas,* a negative regulator of carbon storage that inhibits both starch and lipid accumulation and photosynthetic efficiency under N-starvation in this algae [65]. Expression of this transcript was markedly decreased from the start but increased from 29 hrs starvation on. Differentially expressed transcripts encoding

1830
1831
1832
1833
1834
1835
1836
1837
1838
1839
1840
1841
1842
1843
1844
1845
1846
1847
1848
1849
1850
1851
1852
1853
1854
1855
1856
1857
1858
1859
1860
1861
1862
1863
1864
1865
1866
1867
1868
1869
1870
1871
1872
1873
1874
1875
1876
1877
1878
1879
1880
1881
1882
1883
1884
1885
1886
1887
1888

two homologs of PHR1-like regulators from higher plants were also found (TR19823|c0_g1 and TR25002|c0_g1). PHR1 and its homolog in *Chlamydomonas* PSR1 are Phosphate Starvation Response transcription factors, and PSR1 was found to be essential for lipid and starch accumulation during phosphate starvation in *Chlamydomonas* [66]. A homolog of the nitrogen regulatory protein P-II (GLNB: TR228|c0_g1 and g3) was upregulated from 6 hrs starvation on. The P-II regulator from *Chlamydomonas* was found to negatively control TAG accumulation in lipid bodies during acclimation to nitrogen starvation in this green alga [67]. If and how these regulators affect carbon partitioning for the accumulation of starch and lipids remains to be investigated through functional analysis.

4. Conclusions and discussion

Metabolic engineering of microalgae towards increased lipid or starch productivity requires deeper insight into the genetic details of the metabolic pathways involved and the regulatory mechanisms controlling these pathways. For the oleaginous green microalgae *N. oleoabundans* this genetic information is still very limited, therefore we set out to study the biomass and transcriptional changes that occur upon nitrogen starvation, to find genetic triggers of starch and lipid accumulation in this industrially relevant microalga. Starch and lipid accumulation patterns showed different dynamics over the applied 4-day starvation period. Whereas the starch content increased sharply and peaked within the first day upon nitrogen starvation, lipids (mainly TAG) accumulated more gradually (Supplementary Fig. A.2). A pattern where starch accumulates rapidly ahead of lipid accumulation is observed in other hybrid oleaginous microalgae [9–11]. Starch seems to be the preferred primary storage compound in these species, which is partially due to the fact that its synthesis is biochemically and energetically more favourable than fatty acid biosynthesis [10,68]. On the other hand, lipids have a higher energy

32

density and therefore for the longer term might be the preferred storage compound. Several studies indicate that starch and lipid accumulation are both dependent on *de novo* biosynthesis and therefore competition for common carbon precursors affects carbon-partitioning between starch and lipids. Increasing the carbon precursor supply can thereby be a strategy to influence carbon-partitioning and improve lipid accumulation in some cases [69,70]. Nitrogen starvation also affected the fatty acid composition of the lipid fractions, with a distinctive decrease of the polyunsaturated fatty acids C18:3 and C16:3, concomitant with a large increase of the mono-unsaturated fatty acid C18:1, and small increases of the mono-unsaturated fatty acid C16:1 and the saturated fatty acids C18:0 and C16:0. These changes in fatty acid profile correspond to observations from earlier studies on N-starvation in *N. oleoabundans* [71,72], and was observed in other hybrid oleaginous microalgae as well [9,73]. Besides these metabolic factors, several biosynthetic genes and transcriptional factors have been identified that play a role in accumulation and carbon-partitioning of starch and lipids [6,21,23,53,65]. We therefore determined the transcriptional changes upon N-starvation through RNA-sequencing and observed that gene transcripts for starch- and lipid-related metabolic pathways correlated well with the observed biomass changes. The strong accumulation of starch in the first day could mainly be ascribed to a general increase in transcript abundance for several starch biosynthesis genes. The peak in starch accumulation correlated particularly well with the rapid increase and subsequent decrease in expression of starch synthase genes (SSY2, SSY3, SGG1, SSG2), while the ultimate return to N-replete starch levels also appears to be caused by an increase in transcript levels of different amylase genes (α-, β- and isoamylases) in the later stages.

Expression of fatty acid biosynthesis genes and TAG biosynthesis genes was in general more delayed compared to those for starch biosynthesis and remained at increased levels until 4 days of starvation. Transcripts for the enzymatic reactions performed by PDH, ACS, ACLY and ACCase, which supply the fatty acid biosynthesis precursors acetyl-CoA and malonyl-CoA

1948
1949
1950
1951
1952
1953
1954
1955
1956
1957
1958
1959
1960
1961
1962
1963
1964
1965
1966
1967
1968
1969
1970
1971
1972
1973
1974
1975
1976
1977
1978
1979
1980
1981
1982
1983
1984
1985
1986
1987
1988
1989
1990
1991
1992
1993
1994
1995
1996
1997
1998
1999
2000
2001
2002
2003
2004
2005
2006

respectively, were clearly increased, but especially PDH was constitutively upregulated from 6 to 99 hrs. Likewise, for TAG biosynthesis the genes for G3PDH and glycerol kinase (glycerol-3-phosphate synthesis) and GPAT (incorporation of first acyl chain to glycerol-3-phosphate backbone) were in general up-regulated constitutively from 2 hrs starvation on, while other TAG biosynthesis genes had a more limited time-frame where they showed upregulation. In both pathways (fatty acid and TAG biosynthesis) there appears to be a trend where continuous supply of pathway precursors is important for the gradual accumulation of lipids/TAG. Metabolic engineering of microalgae for increased lipid production has focused on early and late genes in both pathways, either based on the hypothesis that the supply of fatty acid precursors is key for an increased flux through the FA biosynthesis or on the hypothesis that the ultimate conversion(s) steps to TAG are rate-limiting. Effective and ineffective metabolic engineering for increased production of lipids/TAG has been reported for both the first (e.g. [6,74]) and the second approach (e.g., [6,75]), yet it still remains unclear whether the key metabolic nodes for increasing lipid/TAG production are conserved among the plethora of oleaginous microalgae. In this respect, a recent study has demonstrated that overexpression of a native DGAT-2 gene in *N. oleoabundans* can more than double the lipid and TAG content and productivity, as well as alter the saturated fatty acid composition of cells [76]. This indicates that metabolic engineering focused on the final conversion of DAG to TAG is a successful strategy for increased lipid production in *N. oleoabundans*. The DGAT-2 gene that was used for overexpression is not the one showing differential gene expression in our study (TR20062|c0_g1), but another one of the four DGAT-2 genes found in the reference transcriptome (TR12237|c0_g1, g2 and g3). On the other hand, the location of *de novo* TAG biosynthesis remains unclear at this moment. While most of the fatty acid biosynthesis transcripts were predicted to be located in the chloroplast, the subcellular location of the TAG biosynthesis transcripts was variable or unspecified (Supplementary Table 1). Whether TAG

biosynthesis occurs both in the chloroplast and on the endoplasmic reticulum in *N. oleoabundans*, as is the case in many microalgae [77], therefore needs to be verified by further biochemical experimentation.

Several transcriptional regulators have been implicated so far to play a central role in lipid accumulation in microalgae. These include the bZIP-type regulators that are suggested to control several steps of TAG synthesis in *Nannochloropsis* [23], and the nitrogen-responsive regulator (NRR1) and phosphorus stress response regulator (PSR1) in *Chlamydomonas* [21,53]. While these putative switch regulators were identified through transcriptomics and *in silico* studies, the direct role of the *PSR1* gene in lipid accumulation was confirmed by mutagenesis and overexpression. The kinase DYRKP has been implicated to repress both starch and lipid accumulation in *Chlamydomonas* and to result in sustained photosynthetic efficiency under N-starvation [65]. From these described transcriptional regulators, we identified several homologs in *N. oleoabundans* that showed significant differential gene expression upon nitrogen starvation. The actual role of these regulators in starch and lipid accumulation and carbon partitioning now needs to be further analysed through e.g. gene inactivation and gene overexpression approaches.

Finally, it remains unclear whether accumulation of these storage compounds in *N. oleoabundans* is controlled by genetic switches only (i.e. via specific activating or repressing regulators) or that accumulation and carbon partitioning can also be regulated at the metabolic level, e.g. via changes in enzyme quantity or enzyme activity at specific key metabolic nodes. To test these hypotheses, a high-quality genome sequence of *N. oleoabundans* and efficient tools for reverse genetics, such as those for targeted gene knockdown [78] and gene editing [79] in *Nannochloropsis oceanica* will be highly valuable.

2066
2067
2068
2069
2070
2071
2072
2073
2074
2075
2076
2077
2078
2079
2080
2081
2082
2083
2084
2085
2086
2087
2088
2089
2090
2091
2092
2093
2094
2095
2096
2097
2098
2099
2100
2101
2102
2103
2104
2105
2106
2107
2108
2109
2110
2111
2112
2113
2114
2115
2116
2117
2118
2119
2120
2121
2122
2123
2124

Acknowledgements

Author contributions

MHJS and JH conceived, designed and performed all experiments, sample processing and biomass analysis. MHJS, YG and DW performed data processing, analysis and interpretation. JX and RHW acquired funding and supervised the work. MHJS and YG wrote the manuscript. All authors revised the manuscript. All authors read and approved the final manuscript.

References

[1] C.M. Beal, L.N. Gerber, D.L. Sills, M.E. Huntley, S.C. Machesky, M.J. Walsh, J.W. Tester, I. Archibald, J. Granados, C.H. Greene, Algal biofuel production for fuels and feed in a 100-ha facility: A comprehensive techno-economic analysis and life cycle assessment, Algal Res. 10 (2015) 266–279. doi:10.1016/j.algal.2015.04.017.

[2] T.M. Mata, A.A. Martins, N.S. Caetano, Microalgae for biodiesel production and other applications: A review, Renew. Sustain. Energy Rev. 14 (2010) 217–232. doi:10.1016/j.rser.2009.07.020.

[3] B.J. Walsh, F. Rydzak, A. Palazzo, F. Kraxner, M. Herrero, P.M. Schenk, P. Ciais, I.A. Janssens, J. Peñuelas, A. Niederl-Schmidinger, M. Obersteiner, New feed sources key to ambitious climate targets, Carbon Balance Manag. 10 (2015) 26. doi:10.1186/s13021-015-0040-7.

[4] J. Ruiz, G. Olivieri, J. de Vree, R. Bosma, P. Willems, J.H. Reith, M.H.M. Eppink, D.M.M. Kleinegris, R.H. Wijffels, M.J. Barbosa, Towards industrial products from microalgae, Energy Environ. Sci. 9 (2016) 3036–3043. doi:10.1039/C6EE01493C.

[5] R.H. Wijffels, M.J. Barbosa, An outlook on microalgal biofuels., Science. 329 (2010) 796–799. doi:10.1126/science.1189003.

[6] J.A. Gimpel, V. Henríquez, S.P. Mayfield, In Metabolic Engineering of Eukaryotic Microalgae: Potential and Challenges Come with Great Diversity, Front. Microbiol. 6 (2015) 1–14. doi:10.3389/fmicb.2015.01376.

[7] J. Levering, J. Broddrick, K. Zengler, Engineering of oleaginous organisms for lipid production, Curr. Opin. Biotechnol. 36 (2015) 32–39. doi:10.1016/j.copbio.2015.08.001.

[8] E. Poliner, J.A. Pulman, K. Zienkiewicz, K. Childs, C. Benning, E.M. Farre, A toolkit for Nannochloropsis oceanica CCMP1779 enables gene stacking and genetic engineering of the eicosapentaenoic acid pathway for enhanced long-chain polyunsaturated fatty acid production.,

Plant Biotechnol. J. (2017). doi:10.1111/pbi.12772.

[9]   G. Breuer, P.P. Lamers, D.E. Martens, R.B. Draaisma, R.H. Wijffels, The impact of nitrogen

       starvation on the dynamics of triacylglycerol accumulation in nine microalgae strains,

       Bioresour. Technol. 124 (2012) 217–226. doi:10.1016/j.biortech.2012.08.003.

[10]   T. Li, M. Gargouri, J. Feng, J. Park, D. Gao, C. Miao, T. Dong, D.R. Gang, S. Chen,

       Bioresource Technology Regulation of starch and lipid accumulation in a microalga Chlorella

       sorokiniana, Bioresour. Technol. 180 (2015) 250–257. doi:10.1016/j.biortech.2015.01.005.

[11]   T. Takeshita, S. Ota, T. Yamazaki, A. Hirata, V. Zachleder, S. Kawano, Starch and lipid

       accumulation in eight strains of six Chlorella species under comparatively high light intensity

       and aeration culture conditions, Bioresour. Technol. 158 (2014) 127–134.

       doi:10.1016/j.biortech.2014.01.135.

[12]   A.M. Santos, R.H. Wijffels, P.P. Lamers, pH-upshock yields more lipids in nitrogen-starved

       Neochloris oleoabundans, Bioresour. Technol. 152 (2014) 299–306.

       doi:10.1016/j.biortech.2013.10.079.

[13]   A.M. Santos, M. Janssen, P.P. Lamers, W. a C. Evers, R.H. Wijffels, Growth of oil

       accumulating microalga Neochloris oleoabundans under alkaline-saline conditions, Bioresour.

       Technol. 104 (2012) 593–599. doi:10.1016/j.biortech.2011.10.084.

[14]   A.J. Klok, D.E. Martens, R.H. Wijffels, P.P. Lamers, Simultaneous growth and neutral lipid

       accumulation in microalgae, Bioresour. Technol. 134 (2013) 233–243.

       doi:10.1016/j.biortech.2013.02.006.

[15]   L. de Jaeger, Strain Improvement of Oleaginous Microalgae, Wageningen University, 2015.

       http://edepot.wur.nl/357391.

[16]   J. Pruvost, G. Van Vooren, G. Cogne, J. Legrand, Investigation of biomass and lipids

       production with Neochloris oleoabundans in photobioreactor, Bioresour. Technol. 100 (2009)

       5988–5995. doi:10.1016/j.biortech.2009.06.004.

[17] H. Rismani-Yazdi, B.Z. Haznedaroglu, C. Hsin, J. Peccia, Transcriptomic analysis of the oleaginous microalga Neochloris oleoabundans reveals metabolic insights into triacylglyceride accumulation, Biotechnol. Biofuels. 5 (2012) 74. doi:10.1186/1754-6834-5-74.

[18] A.J. Klok, Lipid production in microalgae, Wageningen University, 2013. http://edepot.wur.nl/283092.

[19] A. Klok, Optimization of lipid production in microalgae, n.d.

[20] D. Jaeger, A. Winkler, J.H. Mussgnug, J. Kalinowski, A. Goesmann, O. Kruse, Biotechnology for Biofuels Time ☐ resolved transcriptome analysis and lipid pathway reconstruction of the oleaginous green microalga Monoraphidium neglectum reveal a model for triacylglycerol and lipid hyperaccumulation, Biotechnol. Biofuels. (2017) 1–34. doi:10.1186/s13068-017-0882-1.

[21] C.Y. Ngan, C.-H. Wong, C. Choi, Y. Yoshinaga, K. Louie, J. Jia, C. Chen, B. Bowen, H. Cheng, L. Leonelli, R. Kuo, R. Baran, J.G. García-Cerdán, A. Pratap, M. Wang, J. Lim, H. Tice, C. Daum, J. Xu, T. Northen, A. Visel, J. Bristow, K.K. Niyogi, C.-L. Wei, Lineage-specific chromatin signatures reveal a regulator of lipid metabolism in microalgae, Nat. Plants. 1 (2015) 1–12. doi:10.1038/NPLANTS.2015.107.

[22] J. Fan, K. Ning, X. Zeng, Y. Luo, D. Wang, J. Hu, J. Li, H. Xu, Genomic Foundation of Starch-to-Lipid Switch in Oleaginous Chlorella spp . 1, 169 (2015) 2444–2461. doi:10.1104/pp.15.01174.

[23] J. Hu, D. Wang, J. Li, G. Jing, K. Ning, J. Xu, Genome-wide identification of transcription factors and transcription-factor binding sites in oleaginous microalgae Nannochloropsis, Sci. Rep. 4 (2014) 1–11. doi:10.1038/srep05454.

[24] J. Li, D. Han, D. Wang, K. Ning, J. Jia, L. Wei, X. Jing, S. Huang, J. Chen, Y. Li, Q. Hu, J. Xu, Choreography of Transcriptomes and Lipidomes of Nannochloropsis Reveals the Mechanisms of Oil Synthesis in Microalgae, Plant Cell. 26 (2014) 1645–1665. doi:10.1105/tpc.113.121418.

[25] J. Jia, D. Han, H.G. Gerken, Y. Li, M. Sommerfeld, Q. Hu, J. Xu, Molecular mechanisms for

photosynthetic carbon partitioning into storage neutral lipids in Nannochloropsis oceanica

under nitrogen-depletion conditions, Algal Res. 7 (2015) 66–77.

doi:10.1016/j.algal.2014.11.005.

[26] A.M.J. Kliphuis, A.J. Klok, D.E. Martens, P.P. Lamers, M. Janssen, R.H. Wijffels, Metabolic

modeling of Chlamydomonas reinhardtii: Energy requirements for photoautotrophic growth

and maintenance, J. Appl. Phycol. 24 (2012) 253–266. doi:10.1007/s10811-011-9674-3.

[27] G. Breuer, W.A.C. Evers, J.H. de Vree, D.M.M. Kleinegris, D.E. Martens, R.H. Wijffels, P.P.

Lamers, Analysis of Fatty Acid Content and Composition in Microalgae, J. Vis. Exp. 80 (2013)

e50628. doi:10.3791/50628.

[28] L. de Winter, A.J. Klok, M. Cuaresma Franco, M.J. Barbosa, R.H. Wijffels, The synchronized

cell cycle of Neochloris oleoabundans and its influence on biomass composition under constant

light conditions, Algal Res. 2 (2013) 313–320. doi:10.1016/j.algal.2013.09.001.

[29] R. Edgar, M. Domrachev, A.E. Lash, Gene Expression Omnibus: NCBI gene expression and

hybridization array data repository., Nucleic Acids Res. 30 (2002) 207–210.

[30] A.M. Bolger, M. Lohse, B. Usadel, Trimmomatic: a flexible trimmer for Illumina sequence

data., Bioinformatics. 30 (2014) 2114–2120. doi:10.1093/bioinformatics/btu170.

[31] B.J. Haas, A. Papanicolaou, M. Yassour, M. Grabherr, P.D. Blood, J. Bowden, M.B. Couger,

D. Eccles, B. Li, M. Lieber, M.D. MacManes, M. Ott, J. Orvis, N. Pochet, F. Strozzi, N.

Weeks, R. Westerman, T. William, C.N. Dewey, R. Henschel, R.D. LeDuc, N. Friedman, A.

Regev, De novo transcript sequence reconstruction from RNA-seq using the Trinity platform

for reference generation and analysis, Nat. Protoc. 8 (2013) 1494–1512.

doi:10.1038/nprot.2013.084.

[32] E. Boutet, D. Lieberherr, M. Tognolli, M. Schneider, P. Bansal, A.J. Bridge, S. Poux, L.

Bougueleret, I. Xenarios, UniProtKB/Swiss-Prot, the Manually Annotated Section of the

UniProt KnowledgeBase: How to Use the Entry View., Methods Mol. Biol. 1374 (2016) 23–

54. doi:10.1007/978-1-4939-3167-5_2.

[33]   B.E. Suzek, Y. Wang, H. Huang, P.B. McGarvey, C.H. Wu, UniRef clusters: a comprehensive

        and scalable alternative for improving sequence similarity searches., Bioinformatics. 31 (2015)

        926–932. doi:10.1093/bioinformatics/btu739.

[34]   R.D. Finn, J. Clements, S.R. Eddy, HMMER web server: interactive sequence similarity

        searching., Nucleic Acids Res. 39 (2011) W29-37. doi:10.1093/nar/gkr367.

[35]   M. Punta, P.C. Coggill, R.Y. Eberhardt, J. Mistry, J. Tate, C. Boursnell, N. Pang, K. Forslund,

        G. Ceric, J. Clements, A. Heger, L. Holm, E.L.L. Sonnhammer, S.R. Eddy, A. Bateman, R.D.

        Finn, The Pfam protein families database., Nucleic Acids Res. 40 (2012) D290-301.

        doi:10.1093/nar/gkr1065.

[36]   O. Emanuelsson, H. Nielsen, S. Brunak, G. von Heijne, Predicting subcellular localization of

        proteins based on their N-terminal amino acid sequence., J. Mol. Biol. 300 (2000) 1005–1016.

        doi:10.1006/jmbi.2000.3903.

[37]   B. Langmead, C. Trapnell, M. Pop, S.L. Salzberg, Ultrafast and memory-efficient alignment of

        short DNA sequences to the human genome., Genome Biol. 10 (2009) R25. doi:10.1186/gb-

        2009-10-3-r25.

[38]   B. Li, C.N. Dewey, RSEM: accurate transcript quantification from RNA-Seq data with or

        without a reference genome., BMC Bioinformatics. 12 (2011) 323. doi:10.1186/1471-2105-12-

        323.

[39]   M.D. Robinson, D.J. McCarthy, G.K. Smyth, edgeR: a Bioconductor package for differential

        expression analysis of digital gene expression data., Bioinformatics. 26 (2010) 139–140.

        doi:10.1093/bioinformatics/btp616.

[40]   J. Ye, L. Fang, H. Zheng, Y. Zhang, J. Chen, Z. Zhang, J. Wang, S. Li, R. Li, L. Bolund, J.

        Wang, WEGO: a web tool for plotting GO annotations., Nucleic Acids Res. 34 (2006) W293-7.

        doi:10.1093/nar/gkl031.

41

[41]   M.D. Young, M.J. Wakefield, G.K. Smyth, A. Oshlack, Gene ontology analysis for RNA-seq:
       accounting for selection bias., Genome Biol. 11 (2010) R14. doi:10.1186/gb-2010-11-2-r14.

[42]   A. Conesa, S. Gotz, J.M. Garcia-Gomez, J. Terol, M. Talon, M. Robles, Blast2GO: a universal
       tool for annotation, visualization and analysis in functional genomics research., Bioinformatics.
       21 (2005) 3674–3676. doi:10.1093/bioinformatics/bti610.

[43]   T.Z. Berardini, S. Mundodi, L. Reiser, E. Huala, M. Garcia-Hernandez, P. Zhang, L.A.
       Mueller, J. Yoon, A. Doyle, G. Lander, N. Moseyko, D. Yoo, I. Xu, B. Zoeckler, M. Montoya,
       N. Miller, D. Weems, S.Y. Rhee, Functional annotation of the Arabidopsis genome using
       controlled vocabularies., Plant Physiol. 135 (2004) 745–755. doi:10.1104/pp.104.040071.

[44]   W. Walter, F. Sanchez-Cabo, M. Ricote, GOplot: an R package for visually combining
       expression data with functional analysis., Bioinformatics. 31 (2015) 2912–2914.
       doi:10.1093/bioinformatics/btv300.

[45]   C. Xie, X. Mao, J. Huang, Y. Ding, J. Wu, S. Dong, L. Kong, G. Gao, C.-Y. Li, L. Wei,
       KOBAS 2.0: a web server for annotation and identification of enriched pathways and diseases.,
       Nucleic Acids Res. 39 (2011) W316-22. doi:10.1093/nar/gkr483.

[46]   W. Luo, G. Pant, Y.K. Bhavnasi, S.G.J. Blanchard, C. Brouwer, Pathview Web: user friendly
       pathway visualization and data integration., Nucleic Acids Res. (2017).
       doi:10.1093/nar/gkx372.

[47]   W. Luo, M.S. Friedman, K. Shedden, K.D. Hankenson, P.J. Woolf, GAGE: generally
       applicable gene set enrichment for pathway analysis., BMC Bioinformatics. 10 (2009) 161.
       doi:10.1186/1471-2105-10-161.

[48]   G. Ritte, A. Scharf, N. Eckermann, S. Haebel, M. Steup, Phosphorylation of Transitory Starch
       Is Increased during Degradation 1 [w], 135 (2004) 2068–2077.
       doi:10.1104/pp.104.041301.Under.

[49]   E.C. Goncalves, J. V Johnson, B. Rathinasabapathi, Conversion of membrane lipid acyl groups

to triacylglycerol and formation of lipid bodies upon nitrogen starvation in biofuel green algae Chlorella UTEX29., Planta. 238 (2013) 895–906. doi:10.1007/s00425-013-1946-5.

[50] J.W. Allen, C.C. Dirusso, P.N. Black, Carbon and Acyl chain flux during stress-induced triglyceride accumulation by stable isotopic labeling of the polar microalga Coccomyxa subellipsoidea C169, (2016) 1–29. doi:10.1074/jbc.M116.760843.

[51] K. Yoon, D. Han, Y. Li, M. Sommerfeld, Q. Hu, Phospholipid:Diacylglycerol Acyltransferase Is a Multifunctional Enzyme Involved in Membrane Lipid Turnover and Degradation While Synthesizing Triacylglycerol in the Unicellular Green Microalga Chlamydomonas reinhardtii, Plant Cell. 24 (2012) 3708–3724. doi:10.1105/tpc.112.100701.

[52] X. Liu, L. Ouyang, Z. Zhou, Phospholipid : diacylglycerol acyltransferase contributes to the conversion of membrane lipids into triacylglycerol in Myrmecia incisa during the nitrogen starvation stress, Nat. Publ. Gr. (2016) 1–10. doi:10.1038/srep26610.

[53] N.R. Boyle, M.D. Page, B. Liu, I.K. Blaby, D. Casero, J. Kropat, S.J. Cokus, A. Hong-Hermesdorf, J. Shaw, S.J. Karpowicz, S.D. Gallaher, S. Johnson, C. Benning, M. Pellegrini, A. Grossman, S.S. Merchant, Three Acyltransferases and Nitrogen-responsive Regulator Are Implicated in Nitrogen Starvation-induced Triacylglycerol Accumulation in Chlamydomonas, J. Biol. Chem. 287 (2012) 15811–15825. doi:10.1074/jbc.M111.334052.

[54] L. Wang, W. Shen, M. Kazachkov, G. Chen, Q. Chen, A.S. Carlsson, S. Stymne, R.J. Weselake, J. Zou, Metabolic Interactions between the Lands Cycle and the Kennedy Pathway of Glycerolipid Synthesis in Arabidopsis Developing Seeds, 24 (2012) 4652–4669. doi:10.1105/tpc.112.104604.

[55] P.D. Bates, J. Browse, The Significance of Different Diacylgycerol Synthesis Pathways on Plant Oil Composition and Bioengineering, Front. Plant Sci. 3 (2012) 1–11. doi:10.3389/fpls.2012.00147.

[56] Y. Li-Beisson, F. Beisson, W. Riekhof, Metabolism of acyl-lipids in   Chlamydomonas

43

reinhardtii, 2015. doi:10.1111/tpj.12787.

[57] Y. Li-beisson, B. Shorrosh, F. Beisson, M.X. Andersson, V. Arondel, P.D. Bates, D. Bird, A. Debono, T.P. Durrett, R.B. Franke, I.A. Graham, K. Katayama, A. Kelly, T. Larson, J.E. Markham, M. Miquel, I. Molina, I. Nishida, O. Rowland, K.M. Schmid, H. Wada, R. Welti, C. Xu, R. Zallot, J. Ohlrogge, Acyl-Lipid Metabolism, (2013). doi:10.1199/tab.0161.

[58] J. Warakanont, C.-H. Tsai, E.J.S. Michel, G.R. Murphy, P.Y. Hsueh, R.L. Roston, B.B. Sears, C. Benning, Chloroplast lipid transfer processes in *Chlamydomonas reinhardtii* involving a TRIGALACTOSYLDIACYLGLYCEROL 2 (TGD2) orthologue, Plant J. (2015) n/a-n/a. doi:10.1111/tpj.13060.

[59] K. Shi, Z. Gao, T. Shi, P. Song, L. Ren, H. Huang, Reactive Oxygen Species-Mediated Cellular Stress Response and Lipid Accumulation in Oleaginous Microorganisms : The State of the Art and Future Perspectives, 8 (2017) 1–9. doi:10.3389/fmicb.2017.00793.

[60] Y.M. Zhang, H. Chen, C.L. He, Q. Wang, Nitrogen Starvation Induced Oxidative Stress in an Oil-Producing Green Alga Chlorella sorokiniana C3, PLoS One. 8 (2013) 1–12. doi:10.1371/journal.pone.0069225.

[61] J. Fan, Y. Cui, M. Wan, W. Wang, Y. Li, Lipid accumulation and biosynthesis genes response of the oleaginous Chlorella pyrenoidosa under three nutrition stressors., Biotechnol. Biofuels. 7 (2014) 17. doi:10.1186/1754-6834-7-17.

[62] K. Chokshi, I. Pancha, A. Ghosh, S. Mishra, Biotechnology for Biofuels Nitrogen starvation ☐ induced cellular crosstalk of ROS ☐ scavenging antioxidants and phytohormone enhanced the biofuel potential of green microalga Acutodesmus dimorphus, Biotechnol. Biofuels. (2017) 1–12. doi:10.1186/s13068-017-0747-7.

[63] E. Nukarinen, T. Nägele, L. Pedrotti, B. Wurzinger, E. Baena-gonzalez, W. Dröge-laser, W. Weckwerth, Quantitative phosphoproteomics reveals the role of the AMPK plant ortholog SnRK1 as a metabolic master regulator under energy deprivation, (2016) 1–19.

44

doi:10.1038/srep31697.

[64] R. Ghillebert, E. Swinnen, J. Wen, L. Vandesteene, M. Ramon, K. Norga, F. Rolland, J. Winderickx, The AMPK ∕ SNF1 ∕ SnRK1 fuel gauge and energy regulator : structure , function and regulation, 278 (2011) 3978–3990. doi:10.1111/j.1742-4658.2011.08315.x.

[65] M. Schulz-Raffelt, V. Chochois, P. Auroy, S. Cuiné, E. Billon, D. Dauvillée, Y. Li-Beisson, G. Peltier, Hyper-accumulation of starch and oil in a Chlamydomonas mutant affected in a plant-specific DYRK kinase, Biotechnol. Biofuels. 9 (2016) 55. doi:10.1186/s13068-016-0469-2.

[66] C. Open, A.K. Bajhaiya, A.P. Dean, L.A.H. Zeef, R.E. Webster, J.K. Pittman, PSR1 Is a Global Transcriptional Regulator of Phosphorus De fi ciency Responses and Carbon Storage Metabolism in, 170 (2016) 1216–1234. doi:10.1104/pp.15.01907.

[67] Z. Zalutskaya, N. Kharatyan, K. Forchhammer, E. Ermilova, Reduction of PII signaling protein enhances lipid body production in Chlamydomonas reinhardtii, Plant Sci. 240 (2015) 1–9. doi:10.1016/j.plantsci.2015.08.019.

[68] S. Subramanian, A.N. Barry, S. Pieris, R.T. Sayre, Comparative energetics and kinetics of autotrophic lipid and starch metabolism in chlorophytic microalgae: implications for biomass and biofuel production., Biotechnol. Biofuels. 6 (2013) 150. doi:10.1186/1754-6834-6-150.

[69] J. Fan, K. Ning, X. Zeng, Y. Luo, D. Wang, J. Hu, J. Li, H. Xu, J. Huang, M. Wan, W. Wang, D. Zhang, G. Shen, C. Run, J. Liao, L. Fang, S. Huang, X. Jing, X. Su, A. Wang, L. Bai, Z.M. Hu, J. Xu, Y. Li, Genomic Foundation of Starch to Lipid Switch in Oleaginous Chlorella, Plant Physiol. (2015) pp.01174.2015. doi:10.1104/pp.15.01174.

[70] J. Fan, C. Yan, C. Andre, J. Shanklin, J. Schwender, C. Xu, Oil accumulation is controlled by carbon precursor supply for fatty acid synthesis in Chlamydomonas reinhardtii, Plant Cell Physiol. 53 (2012) 1380–1390. doi:10.1093/pcp/pcs082.

[71] X. Sun, Y. Cao, H. Xu, Y. Liu, J. Sun, D. Qiao, Y. Cao, Effect of nitrogen-starvation, light

45

intensity and iron on triacylglyceride/carbohydrate production and fatty acid profile of

Neochloris oleoabundans HK-129 by a two-stage process, Bioresour. Technol. 155 (2014)

204–212. doi:10.1016/j.biortech.2013.12.109.

[72] H. Rismani-Yazdi, B.Z. Haznedaroglu, C. Hsin, J. Peccia, Transcriptomic analysis of the

oleaginous microalga Neochloris oleoabundans reveals metabolic insights into triacylglyceride

accumulation, Biotechnol. Biofuels. 5 (2012) 74. doi:10.1186/1754-6834-5-74.

[73] S.H. Ho, C.Y. Chen, J.S. Chang, Effect of light intensity and nitrogen starvation on CO 2

fixation and lipid/carbohydrate production of an indigenous microalga Scenedesmus obliquus

CNW-N, Bioresour. Technol. 113 (2012) 244–252. doi:10.1016/j.biortech.2011.11.133.

[74] L. Wei, Q. Wang, Y. Xin, Y. Lu, J. Xu, Enhancing photosynthetic biomass productivity of

industrial oleaginous microalgae by overexpression of RuBisCO activase, Algal Res. 27 (2017)

366–375. doi:https://doi.org/10.1016/j.algal.2017.07.023.

[75] Y. Xin, Y. Lu, Y. Lee, L. Wei, J. Jia, Q. Wang, D. Wang, F. Bai, H. Hu, Q. Hu, J. Liu, Y. Li, J.

Xu, Producing Designer Oils in Industrial Microalgae by Rational Modulation of Co-evolving

Type-2 Diacylglycerol Acyltransferases, Mol. Plant. (2017). doi:10.1016/j.molp.2017.10.011.

[76] P. Klaitong, S. Fa, W. Chungjatupornchai, Accelerated triacylglycerol production and altered

fatty acid composition in oleaginous microalga Neochloris oleoabundans by overexpression of

diacylglycerol, Microb. Cell Fact. (2017) 1–10. doi:10.1186/s12934-017-0677-x.

[77]   a J. Klok, P.P. Lamers, D.E. Martens, R.B. Draaisma, R.H. Wijffels, Edible oils from

microalgae: insights in TAG accumulation., Trends Biotechnol. (2014) 1–8.

doi:10.1016/j.tibtech.2014.07.004.

[78] L. Wei, Y. Xin, Q. Wang, J. Yang, H. Hu, J. Xu, RNAi-based targeted gene knockdown in the

model oleaginous microalgae Nannochloropsis oceanica, Plant J. 89 (2017) 1236–1250.

doi:10.1111/tpj.13411.

[79] Q. Wang, Y. Lu, Y. Xin, L. Wei, S. Huang, J. Xu, Genome editing of model oleaginous

46

microalgae Nannochloropsis spp . by CRISPR / Cas9, Plant J. 88 (2016) 1071–1081.
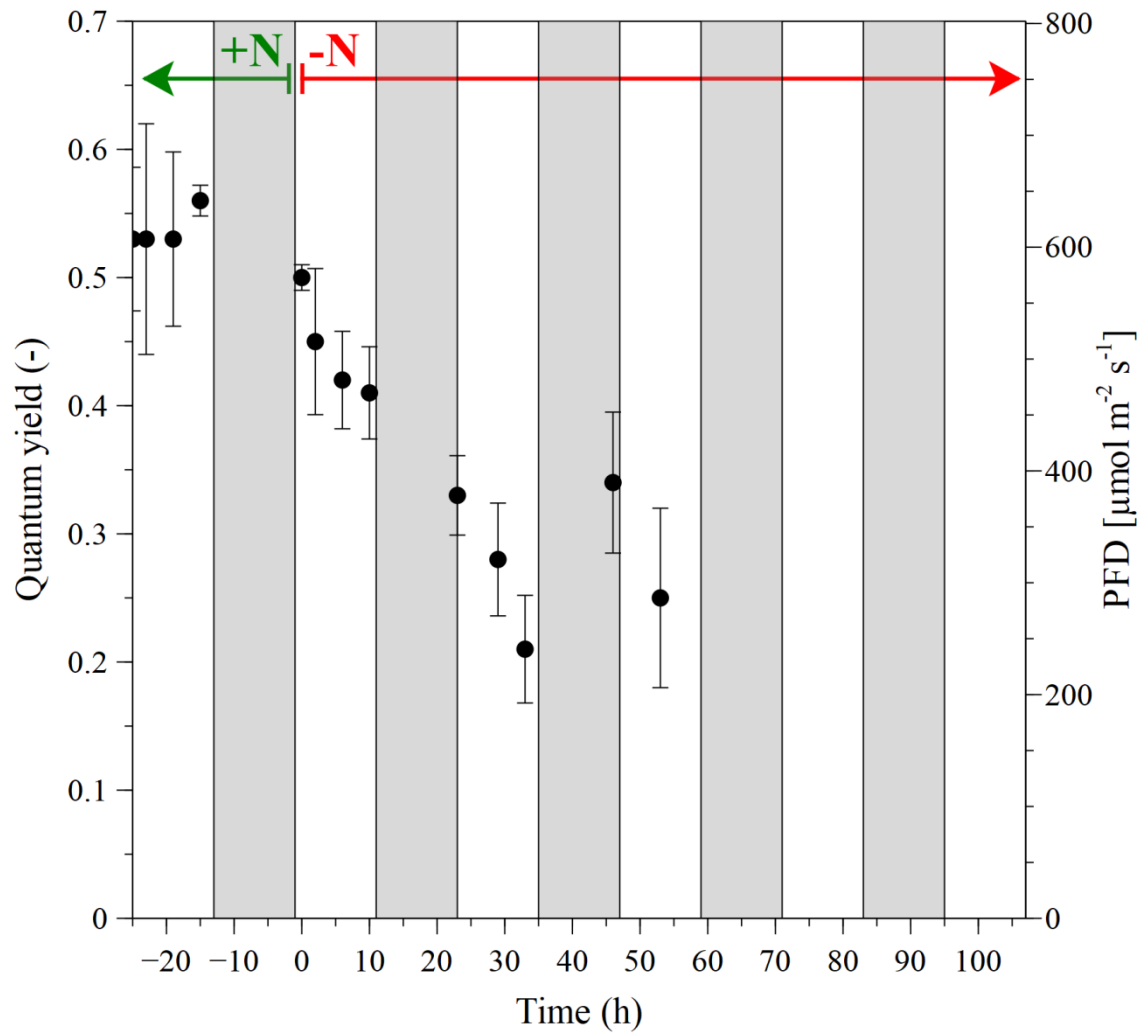
doi:10.1111/tpj.13307.

Acknowledgements

Figure A.1. Quantum yield in *N. oleoabundans* grown in N-replete (+N) and N-starvation (-N) conditions in air-lift flat-panel photobioreactor. Mean values ± standard deviations are shown (n=3). The onset of N-starvation is at t=0h. The 12:12 day-night cycles used for cultivation are shown as alternating 12h light phases (white background) and 12h dark phases (grey background).
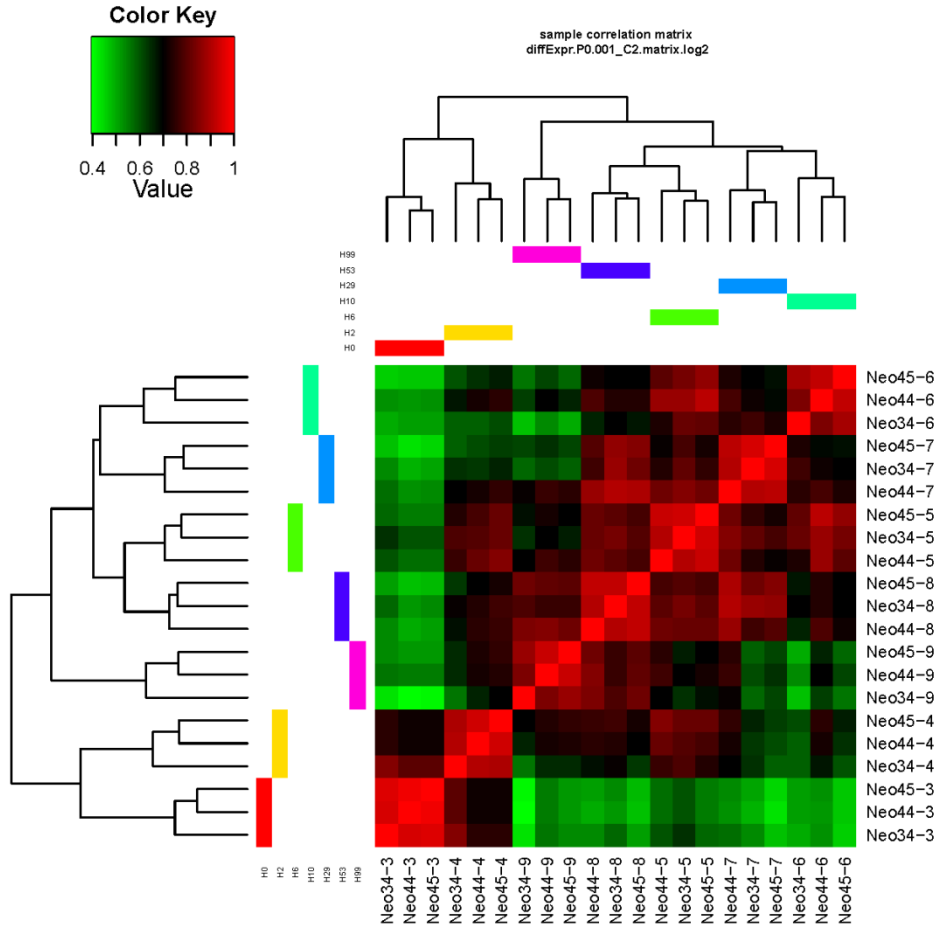
Figure A.2. Sample correlation matrix heatmap of the differential gene expression profiles from triplicate photobioreactor runs. Time points can be clearly separated using hierarchical clustering, indicating a high experimental reproducibility.
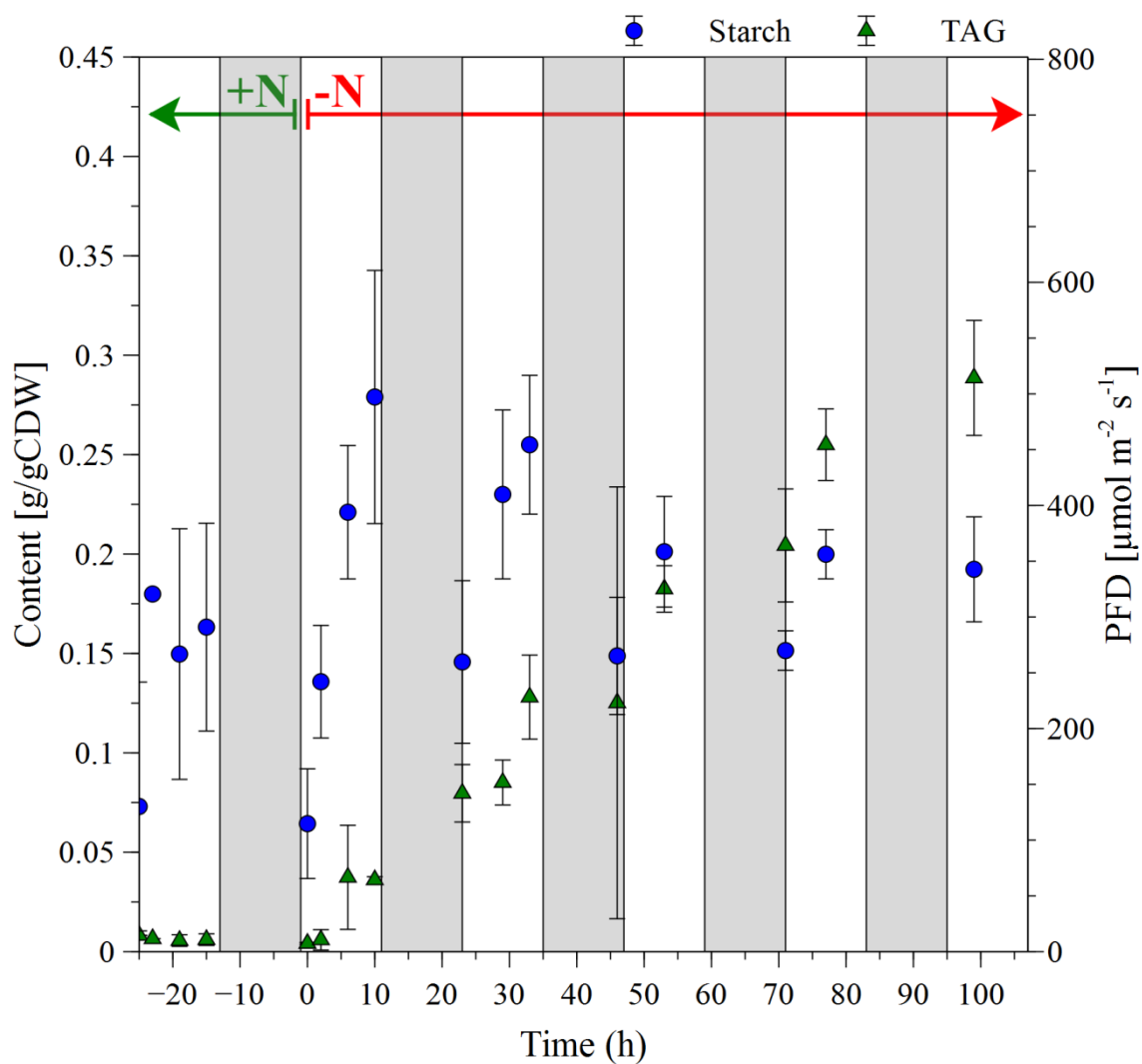
Figure A.3. Starch and triacylglycerides (TAG) content in *N. oleoabundans* grown in N-replete (+N) and N-starvation (-N) conditions in air-lift flat-panel photobioreactor. Mean values ± standard deviations are shown (n=3). The 12:12 day-night cycles used for cultivation are shown as alternating 12h light phases (white background) and 12h dark phases (grey background).
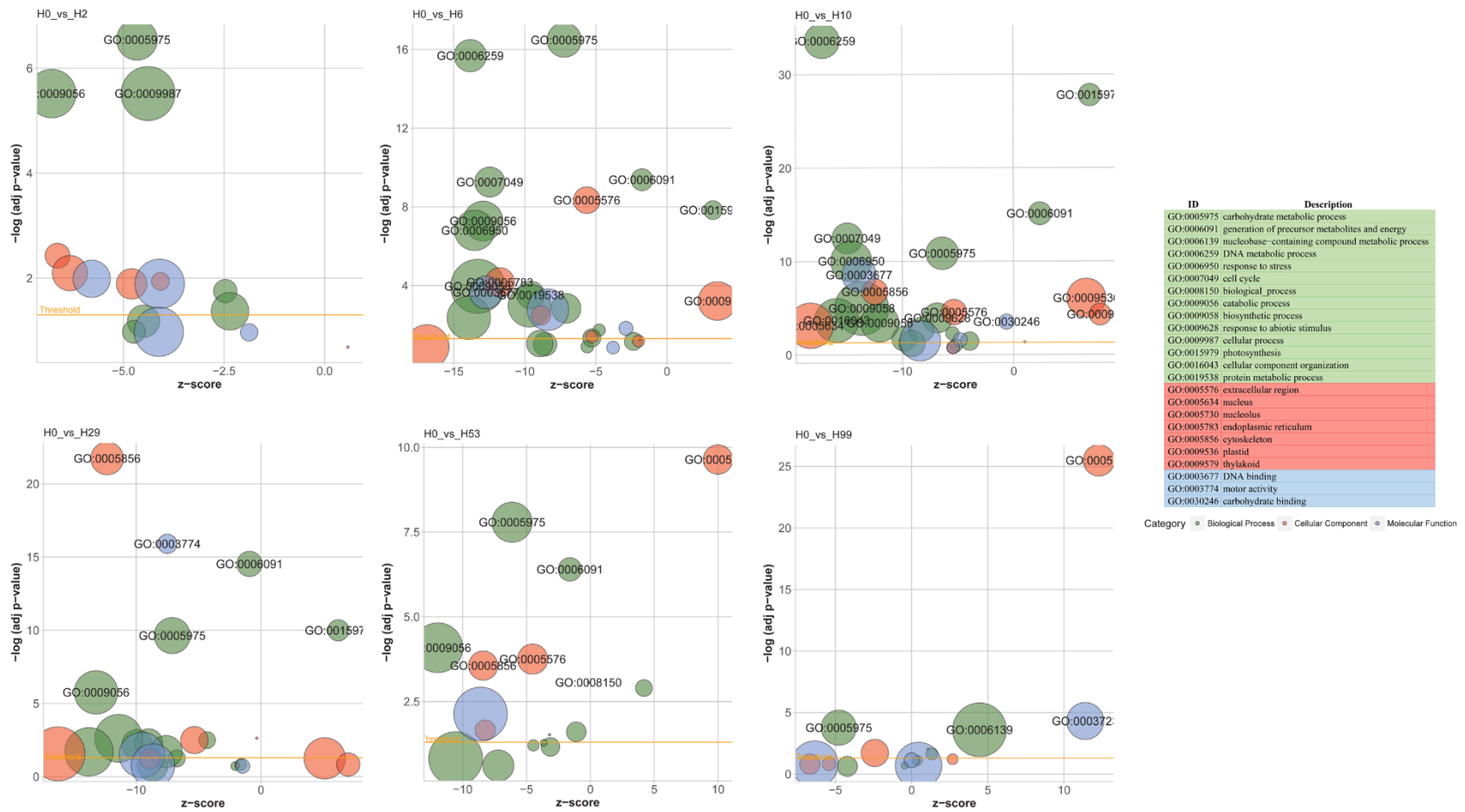
Fig. A.4. GOBubble plots of enriched plant GO Slim terms (compared to H0) in the transcriptome at different timepoints (H2 to H99) for nitrogen-starved *N. oleoabundans*. The *p*-value threshold level is indicated (orange line).